

LLM Serving Optimization with Variable Prefill and Decode Lengths

Meixuan Wang

Department of Computer Science and Technology, Tsinghua University, wangmx22@mails.tsinghua.edu.cn

Yinyu Ye

Department of Management Science and Engineering, Stanford University & Department of Industrial Engineering and Decision Analytics, HKUST, yyye@stanford.edu

Zijie Zhou

Department of Industrial Engineering and Decision Analytics, HKUST, jerryzhou@ust.hk

We study offline scheduling for large language model (LLM) serving under a fixed KV-cache memory budget, where requests have heterogeneous prompt (prefill) and response (decode) lengths. Prompt tokens determine initial KV usage, and each generated token increases memory by one unit. Given a backlog of n requests arriving together, we schedule mixed prefill and decode batches to minimize total end-to-end latency. We show that heterogeneity in prompt lengths makes the problem computationally intractable and that widely used heuristics such as first-come-first-served and shortest-first can be arbitrarily suboptimal. We propose **Sorted-F**, which repeatedly forms feasible batches using a new selection metric that balances batch size against downstream decode cost, and prove it achieves a constant-factor guarantee on total latency. We further develop practical variants—an exact solver for small instances and fast heuristics for larger ones—and evaluate them on a public workload spanning short conversations and long-document summarization, where they consistently reduce average latency relative to standard baselines. Our results highlight that during peak-hour tidal backlogs, greedy GPU packing or short-request prioritization can perform poorly when prompt lengths vary widely, and provide a principled, tunable framework for designing production batch schedulers and planning capacity in memory-constrained LLM serving systems.

1. Introduction

Modern large-scale language models (Brown et al. 2020, Chowdhery et al. 2023, OpenAI 2023) have revolutionized artificial intelligence by demonstrating unprecedented capabilities in natural language generation across diverse linguistic domains and situational contexts. These sophisticated neural networks, trained on extensive corpora of textual data, now serve as foundational components for numerous real-world applications. Their deployment spans conversational agents (Anthropic 2023, OpenAI 2023), information retrieval systems (Microsoft 2023, Google 2023), programming aids (Amazon 2023, GitHub 2021), and even clinical decision support tools (Cascella

et al. 2023, Peng et al. 2023), demonstrating remarkable versatility in professional and consumer domains alike.

Efficient inference represents a fundamental challenge in large language model deployment, focusing on how models process input prompts and generate responses with minimal latency. The inference pipeline consists of two distinct phases. (1) **Prefill**: processing the input prompt (a user-submitted text sequence), and (2) **Decode**: autoregressively generating output tokens (where each token typically corresponds to a word or sub-word unit). Modern LLMs universally employ the Transformer architecture (Vaswani et al. 2017) for this process. For instance, when processing the prompt “Why is the sea blue?”, the model first tokenizes it into discrete units (“Why”, “is”, “the”, “sea”, “blue”, “?”), then sequentially generates output tokens (e.g., beginning with “Because”) while considering both the prompt and previously generated tokens at each step. The core computational challenge emerges in multi-request scenarios, where the system must optimally schedule numerous concurrent inference tasks. This scheduling problem requires careful balancing of computational resources to minimize user-perceived latency, particularly given the autoregressive nature of token generation and the variable length of both input prompts and output responses.

The scheduling problem in LLM inference presents unique challenges that distinguish it from traditional scheduling tasks, primarily due to its dynamic memory constraints. During inference, each computational worker maintains a fixed Key-Value (KV) cache memory capacity, where keys and values represent contextual embeddings derived from both input tokens and autoregressively generated output tokens. The memory capacity depends on the hardware of each worker and the complexity of the LLM used. This memory system exhibits two critical behaviors: (1) it must retain all processed tokens from the prefill input prompt, and (2) its consumption grows linearly during decode generation as each newly generated output token requires additional KV cache allocation. The memory growth pattern creates complex scheduling dynamics when combined with parallel processing requirements. Unlike traditional systems where task resource demands remain static, LLM inference exhibits variable memory pressure - the number of concurrent requests a worker can handle fluctuates dynamically based on each request’s generation progress. This nonlinear relationship between sequence length and memory consumption fundamentally transforms the scheduling task. The challenge is further compounded by the need to balance immediate memory availability against anticipated future demands as generation progresses across multiple concurrent requests.

Jaillet et al. (2025) established a theoretical model for LLM inference scheduling on a single computational worker, proposing a shortest-first scheduling policy that prioritizes requests with fewer

output tokens. Their approach dynamically batches requests while respecting memory constraints, demonstrating both theoretical and numerical effectiveness under the condition of uniform input sizes. However, this condition may not always hold in practice, where workers typically handle mixed workloads (e.g., combining short conversational prompts with lengthy document summarization tasks).

Relaxing this condition fundamentally changes the scheduling problem. With variable prefill input sizes, the relationship between processing time, memory usage, and optimal scheduling becomes significantly more complex. For instance, a request with a large input but small output may consume substantial memory yet finish quickly, while one with a small input but long output may occupy a small memory for an extended period. This trade-off makes prioritization non-trivial, as the previously effective shortest-first heuristic becomes inadequate. In Section 2.3, we formally analyze these challenges and demonstrate that the generalized scheduling problem is NP-hard and that existing algorithms perform poorly without the uniform input size assumption.

1.1. Main Contribution

In this section, we introduce the main contributions and the roadmap of this paper.

Negative Results for Existing Scheduling Algorithms and NP-hardness. In Section 2, we first establish fundamental limitations of current methods by analyzing the model in [Jaillet et al. \(2025\)](#) under realistic conditions. Our key theoretical findings reveal that: (1) without uniform input sizes, both first-come-first-served and shortest-first scheduling yield unbounded competitive ratios (regardless of using output length or total sequence length as the metric), and (2) the general scheduling problem is NP-hard. These results formally justify the need for new scheduling approaches.

Polynomial Time Scheduling Algorithm with Constant Competitive Ratio. In Section 3, we introduce **Sorted-F**, a novel scheduling algorithm that achieves both computational efficiency and provable performance guarantees. The algorithm operates through three key steps: (1) it first evaluates each request using our designed quality metric, which comprehensively considers both input and output characteristics; (2) it then partitions requests into prioritized batches based on this metric; and (3) within each batch, it applies shortest-output-first prioritization. Crucially, we prove that **Sorted-F** maintains a constant competitive ratio of at most 48, independent of problem scale – a significant improvement over existing approaches that suffer from unbounded ratios in general cases. The proof, presented in Section 4, introduces novel techniques for handling variable

input/output sizes, which may be of independent interest and inspire new theoretical analyses for similar scheduling problems.

Approximation Algorithms for Practical Deployment. Since scheduling latency directly impacts overall inference time in production systems, we investigate efficient approximations of `Sorted-F` that maintain its performance benefits while reducing computational overhead. The primary complexity bottleneck in `Sorted-F` lies in its batch partitioning phase based on our quality metric. In Section 5, we analyze three approximation approaches: (1) exact dynamic programming, (2) local swap search, and (3) quantile greedy selection. For each method, we characterize both its theoretical computational complexity and practical applicability, specifying the problem scales where each variant proves to be most effective. These analyses provide system designers with clear guidelines for algorithm selection based on their specific latency requirements and workload characteristics.

LP-based Heuristics. In Section 6, we further analyze the scheduling problem through an optimization lens by formulating it as an Integer Program (IP), as suggested in [Jaillet et al. \(2025\)](#). While this IP provides theoretical optimality, its time complexity makes it impractical for real-time inference systems requiring millisecond-level decisions. Our work makes two key contributions in this direction: first, we discuss the gap between the IP formulation and its LP relaxation; second, we develop `Sorted-LP`, a novel heuristic that leverages the relaxed LP solution structure. `Sorted-LP` operates by (1) solving the LP relaxation, (2) extracting expected starting times from the fractional solution, and (3) sorting requests according to the expected starting times. We also characterize `Sorted-LP`'s advantages and limitations, providing practitioners with clear guidance for algorithm selection.

Numerical Experiments. In Section 7, we present comprehensive empirical evaluations using real-world data to validate our theoretical findings. To accurately capture the practical challenges of variable-length inputs, we construct a mixed dataset combining: (1) short conversational prompts from [Zheng et al. \(2023a\)](#), and (2) long document summarization tasks from [Cohan et al. \(2018\)](#). This experimental design reflects realistic deployment scenarios where LLM servers must handle diverse request types simultaneously. We evaluate four scheduling approaches: first-come-first-served, shortest-first, our LP-based `Sorted-LP`, and our main proposed algorithm `Sorted-F`. The results demonstrate that `Sorted-F` achieves significantly lower average latency, confirming both the theoretical robustness and practical effectiveness of our approach.

1.2. Other Related Works

LLM Inference. Improving the efficiency of LLM inference is crucial due to the substantial computational and financial costs it incurs. A large body of existing work focuses on practical implementation techniques to accelerate inference in deployed systems, often without accompanying theoretical guarantees. For instance, [Patel et al. \(2023\)](#), [Zhong et al. \(2024\)](#) propose system architectures that process prompt and token requests independently, while other works such as [Yu et al. \(2022\)](#), [Agrawal et al. \(2023, 2024b\)](#) introduce designs that jointly handle prompt and token requests—a structure aligned with the one studied in this paper.

In contrast, a few recent studies aim to develop theoretical foundations for LLM inference. The primary mathematical model considered in this paper builds on the framework introduced by [Jaillet et al. \(2025\)](#). [Ao et al. \(2025\)](#) examine inference scheduling under multiple objectives and propose algorithms with provable performance guarantees. Additionally, [Chen et al. \(2025, 2026\)](#) study the scheduling optimization with unknown decode lengths, and [Li et al. \(2025\)](#) analyze the stability conditions of LLM inference when operating on a single computational worker.

Scheduling. The scheduling problem—extensively studied in the literature ([Allahverdi et al. 2008](#), [Chen et al. 1998](#), [Brucker et al. 1999](#), [Albers 2009](#), [Mak et al. 2015](#), [Xing and Zhang 2000](#), [Kong et al. 2013](#))—involves a decision-maker tasked with processing a large number of incoming requests, either one-by-one or in batches. The challenge lies in determining the optimal order and timing of processing, which is often formulated as an integer optimization problem. However, due to the computational complexity and the impracticality of solving large-scale instances exactly, researchers have developed fast approximation algorithms and heuristics.

In our setting, which is motivated by LLM inference, jobs can be processed in batches. This aligns our problem more closely with batch scheduling models studied in ([Brucker et al. 1998](#), [Chen and Lee 2008](#), [Liu and Lu 2015](#), [Li et al. 2020](#)). Furthermore, LLM inference imposes a sequential structure on token generation—future tokens cannot be processed before current ones—introducing a form of precedence constraint. Related work on scheduling with precedence constraints includes ([Shahout et al. 2024](#), [Garg et al. 2019](#), [Azar and Epstein 2002](#), [Robert and Schabanel 2008](#), [Agrawal et al. 2016](#)). Nevertheless, our setting is fundamentally different due to the unique characteristics of the KV cache, which introduces new constraints and tradeoffs not captured by traditional precedence scheduling models.

2. Model Review

In this section, we review the scheduling model introduced by [Jaillet et al. \(2025\)](#) for LLM inference under memory constraints. Before presenting the formal model, we provide background on two key features of modern LLM serving systems—*prefill/decode mixing* and *continuous batching*—that the model captures. We then discuss our extension, which relaxes a strong assumption on input sizes made in the original work.

Prefill/Decode (PD) mixing. Modern LLM serving systems support prefill/decode (PD) mixing [Kwon et al. \(2023\)](#), whereby a single processing batch can simultaneously contain requests in different phases—some undergoing prefill while others are mid-decode. This mixing improves hardware utilization by combining diverse workloads within each batch.

Continuous Batching. Traditional batching forms a fixed set of requests and processes them until all complete before admitting new requests. In contrast, continuous batching dynamically admits new requests into an ongoing batch as soon as memory capacity becomes available—typically when an in-progress request completes and releases its KV cache. This approach significantly improves throughput by avoiding idle capacity while waiting for long-running requests to finish.

Figure 1 illustrates the scheduling process. Circles represent prefill operations and squares represent decode operations, with colors distinguishing requests. Operations aligned vertically form a batch processed in parallel. The figure demonstrates PD mixing (e.g., prefill and decode operations co-occur in the same batch) and continuous batching (new requests enter as earlier ones complete and release memory).

2.1. Mathematical Model Review

[Jaillet et al. \(2025\)](#) introduces a discrete-time system with a single computational worker. The worker has a KV cache capacity of $M > 0$ tokens; in practice, M depends on model size and hardware specifications (e.g., GPU memory) and is assumed known to the scheduler.

Request Arrivals and Adversarial Setting. We consider n prompts that arrive simultaneously at time $t = 0$. Each prompt $i \in [n]$ is characterized by a pair (s_i, o_i) , where s_i denotes the prefill size (number of input tokens) and o_i denotes the number of output tokens to be generated. We adopt an adversarial framework: the adversary selects the number of requests n and the parameters (s_i, o_i) for each request, subject to a scaling constraint described below.

Scaling Assumption. To state asymptotic guarantees as the memory budget M grows, we impose a scaling constraint on the adversary. Define the peak per-request memory as

$$L(M) := \max_{i \in [n]} \{s_i + o_i\}.$$

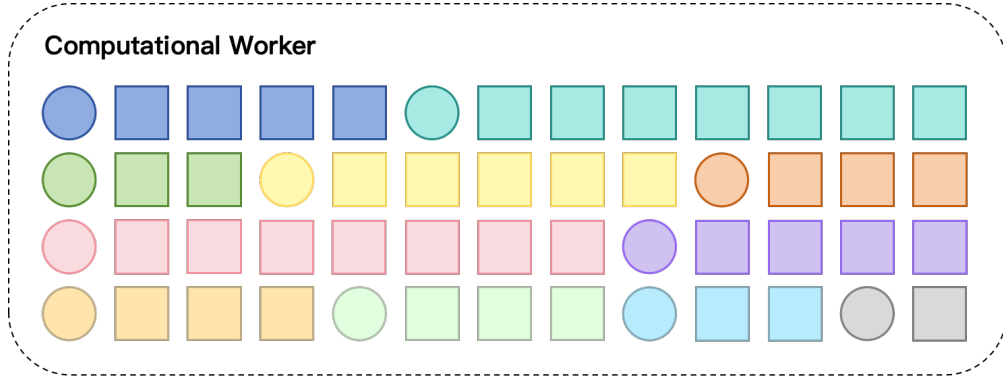


Figure 1 Illustration of LLM inference scheduling with prefill/decode mixing and continuous batching. Circles denote prefill operations; squares denote decode tokens; colors distinguish requests. Operations in the same column constitute a batch processed simultaneously. The schedule exhibits PD mixing (batches contain both prefill and decode operations) and continuous batching (requests enter dynamically as memory becomes available).

We require $L(M) = o(M)$, i.e., $L(M)/M \rightarrow 0$ as $M \rightarrow \infty$. This ensures that each individual request occupies a vanishing fraction of the memory budget, allowing concurrency to grow with hardware capacity.

Justification of the Scaling Assumption. This assumption reflects practical deployment considerations. In real systems, operators first characterize their workload by estimating the rough distribution of prefill and decode lengths for expected requests. They then provision hardware with memory capacity M substantially larger than typical request sizes to achieve high concurrency and throughput. Our scaling assumption $L(M) = o(M)$ captures precisely this regime where hardware is appropriately sized for the workload.

Output Length Information. In the theoretical analysis, we assume that output lengths o_i are known to the scheduler. This assumption isolates the fundamental scheduling challenge, which is already NP-hard (see Section 2.3). In practice, o_i can be predicted, and several effective prediction methods exist (Zheng et al. 2023b, Qiu et al. 2024, Fu et al. 2024, Chen et al. 2024, Shahout et al. 2024). However, none of these prediction methods can guarantee accuracy. In Section 5, we introduce practical methodology that performs well even when prediction accuracy is very poor, rather than relying solely on point estimates.

Batch Processing and Memory Constraint. Each request i must be processed token by token during the decode phase. The memory required to generate the j -th output token ($j \in [o_i]$) is $s_i + j$, reflecting the growing KV cache. At each time step t , the system processes a batch \mathcal{I}_t that may contain tokens from multiple requests at various stages of completion. Consistent with sequential

decoding, at most one token from each request can appear in any batch. The model captures both *PD mixing* (batches combine requests in prefill and decode phases) and *continuous batching* (new requests may join at any time step when capacity permits). The memory constraint requires

$$\sum_{i \in \mathcal{I}_t} (s_i + a_i) \leq M,$$

where a_i is the index of the token from request i in the batch.

Overloaded Regime and Justification of Offline Setting. We restrict attention to overloaded instances where the total workload far exceeds single-batch capacity:

$$\frac{nL(M)}{M} \rightarrow \infty \quad \text{as } M \rightarrow \infty.$$

This restriction is essentially without loss of generality: when n is small that all requests fit into a single batch, they can be processed simultaneously and scheduling becomes trivial. The algorithmic challenge arises precisely when requests must be sequenced across multiple time steps.

This overloaded regime is naturally consistent with the offline arrival model. In practice, LLM inference workloads exhibit *tidal patterns*: request volumes surge during peak hours and subside otherwise. During low-demand periods, requests are served immediately upon arrival, rendering scheduling unnecessary. During peak periods, however, arrivals exceed service capacity, creating a backlog of pending requests that must be prioritized. Our assumption that all n prompts arrive simultaneously at $t = 0$ models this backlogged state during peak demand, and our analysis targets this challenging regime.

2.2. Objective and Performance Metric

The objective is to minimize *total end-to-end latency* (TEL), defined as the sum of completion times. Since all requests arrive at $t = 0$, the latency of request i equals its completion time $c_i(\Lambda)$ under schedule Λ :

$$\text{TEL}(\Lambda; \mathcal{I}) = \sum_{i \in [n]} c_i(\Lambda).$$

Jaillet et al. (2025) formulate an integer linear program (ILP) to compute optimal schedules. However, solving the ILP is computationally prohibitive for real-time deployment, where decisions must be made within milliseconds. Our goal is therefore to design efficient approximation algorithms with provable performance guarantees.

Let **Optimal** denote an optimal schedule for request set \mathcal{I} . The performance of algorithm Λ is measured by its *competitive ratio*:

$$\text{CR}(\Lambda) = \sup_{\mathcal{I}} \frac{\text{TEL}(\Lambda; \mathcal{I})}{\text{TEL}(\text{Optimal}; \mathcal{I})}.$$

The competitive ratio is always at least 1, with smaller values indicating better worst-case performance.

2.3. Challenges with Heterogeneous Input Sizes

Jaillet et al. (2025) propose a *memory-constrained shortest-first* algorithm (MC-SF) that prioritizes requests by output length o_i . Before adding a request to the current batch, the algorithm verifies that memory constraints will remain satisfied at all future time steps.

Formally, let $\mathcal{R}^{(t)}$ denote requests not yet started by time t , and let $S^{(t)}$ denote requests currently in progress (with p_i denoting the start time of request $i \in S^{(t)}$). For a candidate subset $U \subseteq \mathcal{R}^{(t)}$, define $t_{\max}(U) := \max_{i \in U} \{t + o_i\}$. The feasibility condition is:

$$\sum_{i \in S^{(t)}} (s_i + t' - p_i) \cdot \mathbb{1}_{\{o_i \geq t' - p_i\}} + \sum_{i \in U} (s_i + t' - t) \cdot \mathbb{1}_{\{o_i \geq t' - t\}} \leq M, \quad \forall t' \in \{t, \dots, t_{\max}(U)\}. \quad (1)$$

Jaillet et al. (2025) establish strong theoretical and empirical performance of MC-SF under the assumption that $s_i = s$ for all $i \in [n]$. With uniform prefill sizes, shortest-first scheduling is natural: requests with smaller o_i have lower peak memory usage ($s + o_i$) and shorter processing times, so prioritizing them improves both throughput and memory utilization.

However, uniform prefill sizes may not hold when systems handle diverse workloads mixing long and short prompts. Relaxing this assumption introduces fundamental difficulties. Consider requests i and j with $s_i < s_j$ but $o_i > o_j$: request i has lower per-step memory but longer duration, while j has higher memory but finishes quickly. The optimal priority depends on global interactions with other requests, making the trade-off nontrivial.

We show that MC-SF can perform arbitrarily poorly when input sizes vary.

THEOREM 1. *Suppose each request $i \in [n]$ satisfies $s_i \in [1, M]$, $o_i \in [1, M]$, and $s_i + o_i \leq M$. Then MC-SF has unbounded competitive ratio: $\text{CR}(\text{MC-SF}) \rightarrow \infty$ as $M \rightarrow \infty$.*

The proof appears in Appendix EC.1, which also shows that prioritizing by total size $s_i + o_i$ yields an unbounded ratio. Moreover, the problem becomes computationally hard without uniform inputs.¹

THEOREM 2. *Under the model of Jaillet et al. (2025) with $s_i \in [1, M]$, $o_i \in [1, M]$, and $s_i + o_i \leq M$, minimizing total end-to-end latency is NP-hard.*

We prove Theorem 2 via reduction from 3-Partition in Appendix EC.1.

¹ Whether minimizing TEL is NP-hard under uniform s_i remains open.

3. Algorithm Description

This section presents our novel scheduling algorithm designed to minimize total end-to-end latency. The algorithm dynamically schedules requests by balancing memory constraints with a quality metric that optimizes both batch concurrency and response length efficiency.

At the core of our approach is the quality metric $F(\mathcal{X})$ for any request set \mathcal{X} , defined as

$$F(\mathcal{X}) = \frac{\sum_{r_i \in \mathcal{X}} o_i}{|\mathcal{X}|^2},$$

where \mathcal{X} is a set of requests, and $|\mathcal{X}|$ is the cardinality of the request set. Smaller values of $F(\mathcal{X})$ indicate higher scheduling priority. This metric fundamentally improves upon shortest-first methods by naturally balancing batch size and response lengths.

To illustrate its operational intuition, we begin with a concrete numerical example that demonstrates how **Sorted-F** outperforms shortest-first scheduling (**MC-SF**):

EXAMPLE 1. Consider a scenario with KV cache memory $M = 64$ and two request types:

Table 1 Request Types for Memory-Constrained Scheduling

Type	Prompt Size	Response Length	Requests Number
1	63	1	1
2	1	2	21

Under **MC-SF**, which prioritizes shorter outputs, Type 1 would be scheduled first since $o_1 = 1 < o_2 = 2$. After Type 1 completes at time $t = 1$, Type 2 requests are processed in batches. With memory constraint $M = 64$, each batch can accommodate $\lfloor 64 / (1 + 2) \rfloor = 21$ Type 2 requests simultaneously. The total end-to-end latency (TEL) is

$$TEL(\text{MC-SF}; \mathcal{I}) = \underbrace{1}_{\text{Type 1}} + \underbrace{21 \times 3}_{\text{Type 2}} = 64.$$

In contrast, **Sorted-F** computes the F -metric for each type:

$$F(\text{Type 1}) = \frac{1}{1^2} = 1$$

$$F(\text{Type 2}) = \frac{2 \times 21}{21^2} = \frac{42}{441} \approx 0.095.$$

Since $F(\text{Type 2}) < F(\text{Type 1})$, **Sorted-F** prioritizes Type 2 first. Type 2 completes at $t = 2$, after which Type 1 is processed at $t = 3$. The TEL is

$$TEL(\text{Sorted-F}; \mathcal{I}) = \underbrace{21 \times 2}_{\text{Type 2}} + \underbrace{3}_{\text{Type 1}} = 45.$$

This represents a 29.7% reduction in TEL compared to MC-SF, demonstrating how Sorted-F’s F-metric effectively balances batch size and processing time to minimize latency.

Building on this concrete demonstration, we now generalize the intuition through a symbolic example that shows how the F-metric recovers the optimal choice in a stylized setting:

EXAMPLE 2. Consider a simple scenario with two batches of requests where requests are homogeneous within each batch but heterogeneous across batches, as shown in Table 2.

Table 2 Batch Characteristics and Quality Metrics

Batch	Prompt Size	Response Length	Requests Number	Quality Metric
1	s_1	o_1	n_1	o_1/n_1
2	s_2	o_2	n_2	o_2/n_2

Assume that both batches have the same total memory requirement: $n_1(s_1 + o_1) = n_2(s_2 + o_2) = M$. The scheduler must decide which batch to process first.

If batch 1 is prioritized, it completes at time o_1 , contributing o_1n_1 to the total end-to-end latency (TEL). Batch 2 then completes at time $o_1 + o_2$, contributing $o_2n_2 + o_1n_2$ to TEL. Thus, the TEL is $o_1n_1 + o_2n_2 + o_1n_2$.

Conversely, if batch 2 is prioritized, it completes at time o_2 , contributing o_2n_2 to TEL. Batch 1 then completes at time $o_1 + o_2$, contributing $o_1n_1 + o_2n_1$ to TEL. The TEL in this case is $o_1n_1 + o_2n_2 + o_2n_1$.

The difference between the two schedules lies in the cross terms: o_1n_2 versus o_2n_1 . Therefore, if $o_1/n_1 < o_2/n_2$, then $o_1n_2 < o_2n_1$, so prioritizing batch 1 minimizes TEL. Otherwise, prioritizing batch 2 minimizes TEL. This decision rule aligns with selecting the batch with smaller $F(\mathcal{X})$, since $F(\mathcal{X}) = o_i/n_i$ for each batch i .

Examples 1 and 2 illustrate how the F-metric balances batch size and response lengths in scheduling decisions.

A key challenge arises from variability in output sizes: when requests are batched together, they do not necessarily finish processing at the same time. Under our model, once a request completes, its memory resources are freed, allowing new requests to be dynamically added. If output sizes in a batch vary too much, requests finish asynchronously, forcing the scheduler to switch from batch selection to incremental request insertion.

To address this, one useful property—formalized in Lemma 1—ensures that within any selected batch, no single request’s output length dominates the average. This balancing characteristic helps avoid stragglers and also provides analytical leverage in Section 4.

LEMMA 1. *For any batch \mathcal{X} selected in Phase 1, let $o_{\max} = \max_{r_i \in \mathcal{X}} o_i$ and $\bar{o} = \frac{\sum_{r_i \in \mathcal{X}} o_i}{|\mathcal{X}|}$. Then,*

$$\bar{o} > \frac{1}{2} \cdot o_{\max}.$$

Proof of Lemma 1: Let $r_{i_{\max}} \in \arg \max_{r_i \in \mathcal{X}} o_i$ and define $\mathcal{X}^- := \mathcal{X} \setminus \{r_{i_{\max}}\}$. Since \mathcal{X}^- is a feasible subset whenever \mathcal{X} is feasible, the Phase 1 selection rule, minimizing $F(\cdot)$ over feasible subsets, implies

$$F(\mathcal{X}^-) \geq F(\mathcal{X}),$$

i.e.,

$$\frac{\sum_{r_i \in \mathcal{X}} o_i - o_{\max}}{(|\mathcal{X}| - 1)^2} \geq \frac{\sum_{r_i \in \mathcal{X}} o_i}{|\mathcal{X}|^2}.$$

Rearranging the terms yields

$$\frac{\sum_{r_i \in \mathcal{X}} o_i}{|\mathcal{X}|} \geq \frac{|\mathcal{X}|}{2|\mathcal{X}| - 1} \cdot o_{\max} > \frac{1}{2} \cdot o_{\max}.$$

□

After introducing the intuition and a useful property behind the F-metric, we now describe our scheduling algorithm, **Sorted-F**. Let \mathcal{I} denote the set of all requests in the instance. The algorithm has two phases. Phase 1 constructs an ordered list \mathcal{I}' by repeatedly selecting a feasible batch with the smallest $F(\cdot)$, with ties broken by preferring a larger batch. Phase 2 then executes the schedule over discrete timesteps $t = 1, 2, \dots$ by maintaining: pending requests $\mathcal{R}^{(t)}$ (not yet started), active requests $\mathcal{V}^{(t)}$ (started but not yet completed), and newly admitted requests $\mathcal{U}^{(t)}$ (admitted at time t and starting at time t). Each request r_i has a unique start time p_i . The memory consumption at a future timestep t^* is

$$M(\mathcal{X}, t^*) = \sum_{r_i \in \mathcal{X}} (s_i + t^* - p_i) \cdot \mathbf{1}_{\{o_i \geq t^* - p_i\}}.$$

The complete procedure is formalized in Algorithm 1.

In Phase 1, **Sorted-F** iteratively selects batches \mathcal{X}^* that minimize $(F(\mathcal{X}), -|\mathcal{X}|)$ over feasible subsets, i.e., it first minimizes $F(\mathcal{X})$ and breaks ties by preferring a larger batch. The selected requests within each batch are then sorted by nondecreasing o_i , and the resulting ordered batches are concatenated into the ordered list \mathcal{I}' .

In Phase 2, the algorithm executes over timesteps by (i) removing completed requests, (ii) admitting new requests from $\mathcal{R}^{(t-1)}$ in the order induced by \mathcal{I}' as long as the memory feasibility checks remain satisfied, and (iii) generating one token per active request concurrently.

Algorithm 1 Sorted-F

```

1: Phase 1: Batch Construction
2:  $\mathcal{I}' \leftarrow []$ 
3: while  $\mathcal{I} \neq \emptyset$  do
4:    $\mathcal{X}^* \leftarrow \arg \min_{\mathcal{X} \subseteq \mathcal{I}} (F(\mathcal{X}), -|\mathcal{X}|)$ 
      subject to  $M(\mathcal{X}, o_j) \leq M, \forall r_j \in \mathcal{X}$ 
5:   Sort requests in  $\mathcal{X}^*$  in nondecreasing order of  $o_i$ 
6:   Append the ordered list  $\mathcal{X}^*$  to the end of  $\mathcal{I}'$ 
7:    $\mathcal{I} \leftarrow \mathcal{I} \setminus \mathcal{X}^*$ 
8: end while
9: Phase 2: Scheduling Execution
10:  $t \leftarrow 0, \mathcal{R}^{(0)} \leftarrow \mathcal{I}', \mathcal{V}^{(0)} \leftarrow \emptyset$ 
11: while  $\mathcal{R}^{(t)} \neq \emptyset$  or  $\mathcal{V}^{(t)} \neq \emptyset$  do
12:    $t \leftarrow t + 1$ 
13:    $\mathcal{U}^{(t)} \leftarrow \emptyset$ 
14:    $\mathcal{V}^{(t)} \leftarrow \{r_j \in \mathcal{V}^{(t-1)} : p_j + o_j \geq t\}$ 
15:   for  $r_i \in \mathcal{R}^{(t-1)}$  in order do
16:     tentatively set  $p_i \leftarrow t$ 
17:      $\widehat{\mathcal{U}} \leftarrow \mathcal{U}^{(t)} \cup \{r_i\}$ 
18:     if  $M(\mathcal{V}^{(t)} \cup \widehat{\mathcal{U}}, p_j + o_j) \leq M, \forall r_j \in \mathcal{V}^{(t)} \cup \widehat{\mathcal{U}}$  then
19:        $\mathcal{U}^{(t)} \leftarrow \widehat{\mathcal{U}}$ 
20:     else
21:       break
22:     end if
23:   end for
24:    $\mathcal{R}^{(t)} \leftarrow \mathcal{R}^{(t-1)} \setminus \mathcal{U}^{(t)}$ 
25:    $\mathcal{V}^{(t)} \leftarrow \mathcal{V}^{(t)} \cup \mathcal{U}^{(t)}$ 
26:   PROCESSONESTEP( $\mathcal{V}^{(t)}$ )
27: end while

```

4. Proof of Constant Competitive Ratio

In this section, we prove the following theorem:

THEOREM 3. *Sorted-F achieves a constant competitive ratio upper bounded by 48 against the optimal schedule *Optimal*, i.e.,*

$$\text{CR}(\text{Sorted-F}) < 48.$$

To prove Theorem 3, we transform **Sorted-F** sequentially: **Sorted-F** \rightarrow **Sorted-F_{separate}** (Theorem 4) \rightarrow **Sorted-F_{group}** (Theorem 5) \rightarrow **Sorted-F_{align}** (Theorem 6). At each step, we deliberately modify the schedule's structure, but crucially, we prove that the cumulative latency increase remains within constant factors. In parallel, we restructure **Optimal** into **Optimal_{align}** (Theorem 7). The proof culminates in a direct comparison between **Sorted-F_{align}** and **Optimal_{align}** (Theorem 8). For clarity, we state each transformation as a self-contained mathematical definition (Definitions 1–5). Figures 2–5 are schematic illustrations of these definitions and are not used as substitutes for the formal constructions.

REMARK 1 (INTERMEDIATE SCHEDULES AND FEASIBILITY). *All schedules introduced in the proof as transformations of **Sorted-F** or **Optimal** (e.g., **Sorted-F_{separate}**, **Sorted-F_{group}**, **Sorted-F_{align}**, and **Optimal_{align}**) are analytical intermediates used only to compare TEL values. They are not meant to represent executable schedules and may violate the memory constraint. Whenever the budget M appears, it is invoked solely to exploit structural properties of the original feasible schedules **Sorted-F** and **Optimal** (e.g., saturation/efficiency facts), rather than to claim feasibility of the intermediates.*

We now begin the first step of the proof. Let $\{\mathcal{X}_k\}$ denote the sequence of batches iteratively generated in Phase 1 of **Sorted-F**. Let the requests in \mathcal{X}_k , ordered by increasing response length, be denoted as $r_{k,1}, r_{k,2}, \dots, r_{k,n_k}$, where $n_k = |\mathcal{X}_k|$.

DEFINITION 1 (SEPARATION TRANSFORMATION **Sorted-F \mapsto **Sorted-F_{separate}**).** *Fix the batch sequence $\{\mathcal{X}_k\}_{k \geq 1}$ produced by Phase 1 of **Sorted-F**. Let $p_{k,j}$ be the initiation time of request $r_{k,j} \in \mathcal{X}_k$ under **Sorted-F**. We construct **Sorted-F_{separate}** by (i) enforcing no inter-batch overlap, (ii) enforcing simultaneous initiation within each batch, and (iii) making consecutive batches tight (i.e., no idle gap between them).*

Define recursively:

$$B_1 := \max_{1 \leq j \leq n_1} p_{1,j}, \quad p'_{1,j} := B_1, \quad j = 1, \dots, n_1, \quad C'_1 := \max_{1 \leq j \leq n_1} \{p'_{1,j} + o_{1,j}\}.$$

For each $k \geq 2$, set

$$B_k := C'_{k-1}, \quad p'_{k,j} := B_k, \quad j = 1, \dots, n_k, \quad C'_k := \max_{1 \leq j \leq n_k} \{p'_{k,j} + o_{k,j}\}.$$

Thus all requests in \mathcal{X}_k start simultaneously at time B_k , and batch k starts exactly when batch $k-1$ finishes, i.e., $B_k = C'_{k-1}$ for all $k \geq 2$.

The transformation in Definition 1 is schematically illustrated in Figure 2.

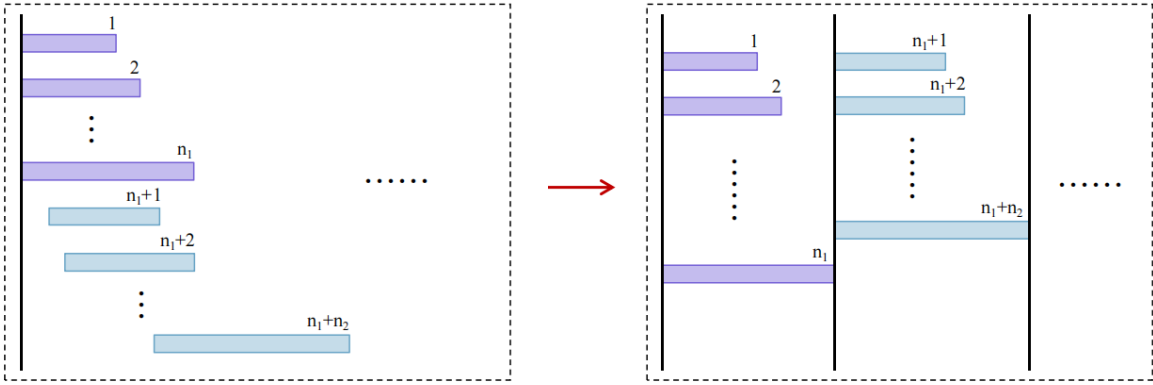


Figure 2 Schematic illustration of Definition 1 (from Sorted-F to Sorted-F_{separate}). The horizontal axis is time; each block represents a request whose width equals its response length.

Theorem 4 characterizes the relationship between the total end-to-end latency of Sorted-F and that of Sorted-F_{separate}.

THEOREM 4. For any \mathcal{I} , the total end-to-end latency of Sorted-F is bounded above by that of Sorted-F_{separate}, i.e.,

$$\text{TEL}(\text{Sorted-F}; \mathcal{I}) \leq \text{TEL}(\text{Sorted-F}_{\text{separate}}; \mathcal{I}).$$

Let $p_{k,j}$ and $p'_{k,j}$ denote the initiation times of request $r_{k,j}$ under Sorted-F and Sorted-F_{separate}, respectively. It suffices to show

$$p_{k,j} \leq p'_{k,j} \quad \forall k \geq 1, \quad \forall j \in \{1, \dots, n_k\}, \quad (2)$$

since response lengths are unchanged.

We first show that **Sorted-F** has no idle gap between consecutive Phase 1 batches: for every $k \geq 2$,

$$\max_{1 \leq j \leq n_k} p_{k,j} \leq \max_{1 \leq j \leq n_{k-1}} (p_{k-1,j} + o_{k-1,j}). \quad (3)$$

Let $T_{k-1} := \max_{1 \leq j \leq n_{k-1}} (p_{k-1,j} + o_{k-1,j})$. If $\max_j p_{k,j} > T_{k-1}$, let $r_{k,\ell}$ be the first request in \mathcal{X}_k (in the Phase 1 order) with $p_{k,\ell} > T_{k-1}$. Then $r_{k,\ell}$ is still pending at time T_{k-1} . However, at each timestep Phase 2 scans \mathcal{I}' in order and admits the longest feasible prefix; at time T_{k-1} all requests in \mathcal{X}_{k-1} have completed, which can only relax the feasibility checks. Since \mathcal{X}_k is feasible in Phase 1 (Algorithm 1, lines 3–4) and feasibility is monotone under taking subsets, $r_{k,\ell}$ must be admissible no later than T_{k-1} , a contradiction. This proves (3).

We now verify (2). For $k = 1$, Definition 1 sets $p'_{1,j} = B_1 = \max_{j'} p_{1,j'} \geq p_{1,j}$. For $k \geq 2$, Definition 1 sets $p'_{k,j} = B_k = C'_{k-1}$ for all j , where

$$C'_{k-1} = \max_{1 \leq j \leq n_{k-1}} \{p'_{k-1,j} + o_{k-1,j}\}.$$

Since $p'_{k-1,j} = B_{k-1} \geq p_{k-1,j}$, we have

$$C'_{k-1} \geq \max_{1 \leq j \leq n_{k-1}} (p_{k-1,j} + o_{k-1,j}) \geq \max_{1 \leq j \leq n_k} p_{k,j},$$

where the last inequality is (3). Hence $p_{k,j} \leq p'_{k,j}$ for all k, j , proving the theorem. \square

DEFINITION 2. A batch \mathcal{X}_k nearly saturates memory M if

$$\sum_{r_i \in \mathcal{X}_k} (s_i + o_i) > M - L(M),$$

where $L(M) := \max_{i \in [n(M)]} \{s_i + o_i\} = o(M)$ is the peak per-request memory defined in Section 2.

THEOREM 5. For any \mathcal{I} , there exists a grouping strategy **Sorted-F**_{group} that aggregates $\{\mathcal{X}_k\}$ into larger groups $\{\mathcal{Y}_m\}$ such that the terminal batch of each group nearly saturates memory M . Additionally, the total end-to-end latency of **Sorted-F**_{separate} is bounded above by

$$\text{TEL}(\text{Sorted-F}_{\text{separate}}; \mathcal{I}) < 4 \cdot \text{TEL}(\text{Sorted-F}_{\text{group}}; \mathcal{I}).$$

DEFINITION 3 (GROUPING TRANSFORMATION **Sorted-F_{separate} \mapsto **Sorted-F**_{group}).** Given an increasing index sequence $0 = b_0 < b_1 < b_2 < \dots$, define grouped workloads

$$\mathcal{Y}_m = \mathcal{X}_{b_{m-1}+1} + \mathcal{X}_{b_{m-1}+2} + \dots + \mathcal{X}_{b_m},$$

where “+” means concurrent initiation (analytically) of all requests from the constituent batches. Formally, let $p'_{k,j}$ be the initiation times in $\text{Sorted-F}_{\text{separate}}$. For each group m , set the group anchor time as $\tau_m := \min_{1 \leq j \leq n_{b_{m-1}+1}} p'_{b_{m-1}+1,j}$, and for every batch $k \in \{b_{m-1} + 1, \dots, b_m\}$, shift all its requests by the same amount so that its earliest initiation aligns to τ_m . The resulting initiation times define $\text{Sorted-F}_{\text{group}}$.

Figure 3 schematically illustrates Definition 3.

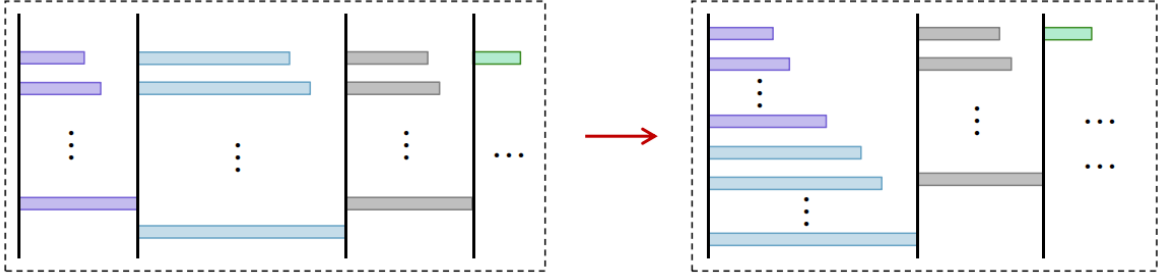


Figure 3 Schematic illustration of Definition 3 (from $\text{Sorted-F}_{\text{separate}}$ to $\text{Sorted-F}_{\text{group}}$).

Proof of Theorem 5: Each group \mathcal{Y}_m is constructed such that b_m is the smallest integer $k > b_{m-1}$ satisfying the inequality

$$\frac{\sum_{j=1}^{n_k} o_{k,j} + o_{k+1,1}}{(n_k + 1)^2} \leq \frac{\sum_{j=1}^{n_k} o_{k,j}}{n_k^2},$$

which implies that including $r_{b_m+1,1}$ in \mathcal{X}_{b_m} would violate the memory constraint M . If this were not the case, the request $r_{b_m+1,1}$ should have been incorporated into \mathcal{X}_{b_m} to either reduce the objective value $F(\mathcal{X}_{b_m})$ or increase the batch size $|\mathcal{X}_{b_m}|$ while preserving $F(\mathcal{X}_{b_m})$. However, such inclusion would contradict the optimal selection criterion of Sorted-F . We therefore conclude that \mathcal{X}_{b_m} must nearly saturate the memory M according to Definition 2.

Next, we quantify how the processing times (i.e., the maximum response length within a batch) decay across batches inside each group. This is captured by the following lemma.

LEMMA 2. For any group \mathcal{Y}_m and any batch index $i \in \{1, \dots, a_m\}$, the longest processing time $o_{b_{m-1}+i, n_{b_{m-1}+i}}$ of batch $\mathcal{X}_{b_{m-1}+i}$ satisfies

$$o_{b_{m-1}+i, n_{b_{m-1}+i}} \leq \left(\frac{1}{2}\right)^{\lfloor \frac{a_m-i}{2} \rfloor} \cdot o_{b_m, n_{b_m}},$$

where $o_{b_m, n_{b_m}}$ is the longest processing time in the terminal batch \mathcal{X}_{b_m} of group \mathcal{Y}_m .

The proof of Lemma 2 appears in Appendix EC.2. By Lemma 2, we obtain

$$\sum_{i=1}^{a_m} o_{b_{m-1}+i, n_{b_{m-1}+i}} \leq \sum_{i=1}^{a_m} \left(\frac{1}{2}\right)^{\lfloor \frac{a_m-i}{2} \rfloor} \cdot o_{b_m, n_{b_m}} \leq 2 \cdot \frac{1 - \left(\frac{1}{2}\right)^{\lfloor \frac{a_m-1}{2} \rfloor}}{1 - \frac{1}{2}} \cdot o_{b_m, n_{b_m}} \leq 4 \cdot o_{b_m, n_{b_m}}. \quad (4)$$

At this point, it remains to convert (4) into a TEL comparison. We rewrite $\text{TEL}(\text{Sorted-F}_{\text{group}}; \mathcal{I})$ and $\text{TEL}(\text{Sorted-F}_{\text{separate}}; \mathcal{I})$ in batch form, regroup by $\{\mathcal{Y}_m\}$, and apply (4) to bound each group's contribution. The next lemma formalizes this bookkeeping step.

LEMMA 3. For any \mathcal{I} ,

$$\text{TEL}(\text{Sorted-F}_{\text{group}}; \mathcal{I}) > \frac{1}{4} \cdot \text{TEL}(\text{Sorted-F}_{\text{separate}}; \mathcal{I}).$$

The proof of Lemma 3 is deferred to Appendix EC.2. Applying Lemma 3 yields $\text{TEL}(\text{Sorted-F}_{\text{separate}}; \mathcal{I}) < 4 \cdot \text{TEL}(\text{Sorted-F}_{\text{group}}; \mathcal{I})$, completing the proof of Theorem 5. \square

DEFINITION 4 (ALIGNMENT TRANSFORMATION $\text{Sorted-F}_{\text{group}} \mapsto \text{Sorted-F}_{\text{align}}$). Consider the terminal batches $\{\mathcal{X}_{b_m}\}$ induced by the grouping in $\text{Sorted-F}_{\text{group}}$. For each terminal batch \mathcal{X}_{b_m} with requests $\{r_{b_m,1}, \dots, r_{b_m, n_{b_m}}\}$, define its average response length

$$\bar{o}_{b_m} = \frac{1}{n_{b_m}} \sum_{i=1}^{n_{b_m}} o_{b_m, i}.$$

The analytically aligned schedule $\text{Sorted-F}_{\text{align}}$ keeps the same initiation times as $\text{Sorted-F}_{\text{group}}$, but replaces every response length in each terminal batch \mathcal{X}_{b_m} by \bar{o}_{b_m} (all non-terminal batches remain unchanged).

Figure 4 schematically illustrates Definition 4.



Figure 4 Schematic illustration of Definition 4 (from $\text{Sorted-F}_{\text{group}}$ to $\text{Sorted-F}_{\text{align}}$).

Theorem 6 compares the total end-to-end latency of $\text{Sorted-F}_{\text{align}}$ with $\text{Sorted-F}_{\text{group}}$.

THEOREM 6. For any \mathcal{I} , the total end-to-end latency of *Sorted-F_{group}* is bounded above by

$$\text{TEL}(\text{Sorted-F}_{\text{group}}; \mathcal{I}) < 2 \cdot \text{TEL}(\text{Sorted-F}_{\text{align}}; \mathcal{I}).$$

Proof of Theorem 6: By Lemma 1,

$$\bar{o}_{b_m} > \frac{1}{2} \cdot o_{b_m, n_{b_m}}.$$

Subsequently, given any \mathcal{I} ,

$$\begin{aligned} \text{TEL}(\text{Sorted-F}_{\text{align}}; \mathcal{I}) &= \sum_{m=1}^{\infty} \left(\bar{o}_{b_m} \cdot \sum_{k=b_m+1}^{\infty} n_k \right) + \sum_{k=1}^{\infty} \sum_{i=1}^{n_k} o_{k,i} \\ &> \sum_{m=1}^{\infty} \left(\frac{1}{2} \cdot o_{b_m, n_{b_m}} \cdot \sum_{k=b_m+1}^{\infty} n_k \right) + \sum_{k=1}^{\infty} \sum_{i=1}^{n_k} o_{k,i} \\ &\geq \frac{1}{2} \cdot \left(\sum_{m=1}^{\infty} \left(o_{b_m, n_{b_m}} \cdot \sum_{k=b_m+1}^{\infty} n_k \right) + \sum_{k=1}^{\infty} \sum_{i=1}^{n_k} o_{k,i} \right) \\ &= \frac{1}{2} \cdot \text{TEL}(\text{Sorted-F}_{\text{group}}; \mathcal{I}). \end{aligned}$$

□

By definition 2, we derive a lower bound on the average memory utilization efficiency η_m for any group \mathcal{Y}_m :

$$\eta_m \geq \frac{\sum_{r_i \in \mathcal{Y}_m} (2s_i + o_i)}{2M} > \frac{M - L(M)}{2M} \rightarrow \frac{1}{2}. \quad (5)$$

Now, we introduce Theorem 7 to construct a lower bound of the total end-to-end latency of *Optimal*.

THEOREM 7. For any \mathcal{I} , there exists a transformed schedule *Optimal_{align}* with time-window scaling and response-length aligning that satisfies

$$\text{TEL}(\text{Optimal}_{\text{align}}; \mathcal{I}) \leq 6 \cdot \text{TEL}(\text{Optimal}; \mathcal{I}).$$

DEFINITION 5 (TIME-WINDOW SCALING AND RESPONSE-LENGTH ALIGNING *Optimal* \mapsto *Optimal_{align}*).

Let *Optimal* have initiation times $\{p_i\}$ and response lengths $\{o_i\}$. We construct *Optimal_{align}* in three steps.

(i) Temporal grouping. Define $\mathcal{A}_1 := \{r_i : p_i = 0\}$ and

$$\delta_1 := \max\{p_i + o_i \mid r_i \in \mathcal{A}_1\}, \quad \mathcal{Z}_1 := \{r_i \in \mathcal{I} \mid p_i + o_i \leq \delta_1\}.$$

For $g \geq 2$, let $S_{g-1} := \sum_{j=1}^{g-1} \delta_j$ and let \mathcal{A}_g be the set of requests initiated but not yet completed by time S_{g-1} . Define

$$\delta_g := \max\{p_i + o_i \mid r_i \in \mathcal{A}_g\} - S_{g-1}, \quad \mathcal{Z}_g := \{r_i \in \mathcal{I} \mid S_{g-1} < p_i + o_i \leq S_{g-1} + \delta_g\}.$$

(ii) Time-window scaling. For each $g \geq 2$, shift all requests in \mathcal{Z}_g forward by $5 \cdot \sum_{j=2}^{g-1} \delta_j$ time units, preserving the within-group relative timing. Define the (scaled) cutting time

$$t_g := 6 \cdot \sum_{j=2}^{g-1} \delta_j,$$

with the convention that an empty sum equals 0.

(iii) Batching + response-length aligning. Within each (shifted) group \mathcal{Z}_g , sort requests by their (shifted) initiation times and greedily partition them into batches

$$\mathcal{Z}_g = \mathcal{W}_{d_{g-1}+1} + \cdots + \mathcal{W}_{d_g},$$

where each batch \mathcal{W}_h is the maximal prefix (in this order) whose total memory requirement does not exceed M . Hence, all batches except possibly the final one in each group nearly saturate memory M by Definition 2. Finally, for each batch \mathcal{W}_h with n_h requests and response lengths $\{o_{h,i}\}_{i=1}^{n_h}$, replace all response lengths in the batch by the average

$$\bar{o}_h := \frac{1}{n_h} \sum_{i=1}^{n_h} o_{h,i}.$$

We denote the resulting analytically transformed schedule by $\text{Optimal}_{\text{align}}$.

Figure 5 schematically illustrates Definition 5.

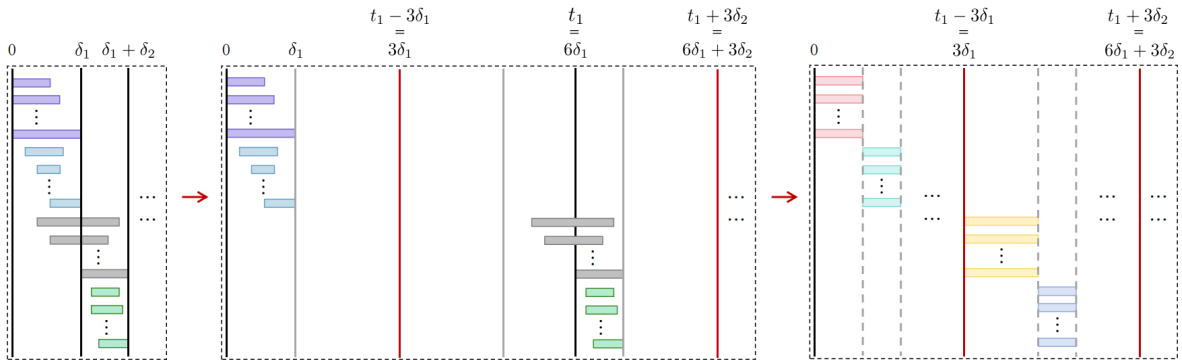


Figure 5 Schematic illustration of Definition 5 (from Optimal to $\text{Optimal}_{\text{align}}$).

Proof of Theorem 7: We now prove $\text{TEL}(\text{Optimal}_{\text{align}}; \mathcal{I}) \leq 6 \cdot \text{TEL}(\text{Optimal}; \mathcal{I})$.

For group \mathcal{Z}_g , let Δt_g denote its original execution window length under **Optimal**:

$$\Delta t_g := \max_{r_i \in \mathcal{Z}_g} (p_i + o_i) - \min_{r_i \in \mathcal{Z}_g} p_i.$$

By construction of $\{\mathcal{Z}_g\}$ (Definition 5(i)), all requests in \mathcal{Z}_g complete no later than $S_{g-1} + \delta_g$, while \mathcal{A}_g contains requests alive at time S_{g-1} ; in particular, $\max_{r_i \in \mathcal{A}_g} (p_i + o_i) = S_{g-1} + \delta_g$. This implies the crude bound $\Delta t_g < \delta_{g-1} + \delta_g$, which is the only property we will use.

By Definition 2, every non-final batch \mathcal{W}_h (i.e., $h \neq d_g$ within its group) satisfies

$$\eta_h \geq \frac{\sum_{r_i \in \mathcal{W}_h} (2s_i + o_i)}{2M} > \frac{M - L(M)}{2M} \rightarrow \frac{1}{2}. \quad (6)$$

Using (6) and the window bound $\Delta t_g < \delta_{g-1} + \delta_g$, the main batches $\mathcal{W}_{d_{g-1}+1}, \dots, \mathcal{W}_{d_g-1}$ complete within $2(\delta_{g-1} + \delta_g)$ time units. The final batch \mathcal{W}_{d_g} has all (aligned) response lengths bounded by $\delta_{g-1} + \delta_g$, hence completes within $\delta_{g-1} + \delta_g$ time units. Therefore, the whole batch sequence of group g finishes within $[t_g - 3\delta_{g-1}, t_g + 3\delta_g]$, where t_g is the scaled cutting time in Definition 5(ii).

It remains to convert the above window bound into a TEL bound. We rewrite $\text{TEL}(\text{Optimal}_{\text{align}}; \mathcal{I})$ in batch form, regroup by $\{\mathcal{Z}_g\}$, and use that group g completes within $[t_g - 3\delta_{g-1}, t_g + 3\delta_g]$. The next lemma formalizes this bookkeeping step.

LEMMA 4. *Given the transformed schedule $\text{Optimal}_{\text{align}}$ constructed in Definition 5, we have*

$$\text{TEL}(\text{Optimal}_{\text{align}}; \mathcal{I}) \leq 6 \cdot \text{TEL}(\text{Optimal}; \mathcal{I}).$$

The proof of Lemma 4 is deferred to Appendix EC.2. Applying Lemma 4 completes the proof of Theorem 7. \square

Finally, Theorem 8 provides the critical linkage between **Sorted-F_{align}** and **Optimal_{align}**.

THEOREM 8. *For any \mathcal{I} , the total end-to-end latency of **Sorted-F_{align}** is upper bounded by the total end-to-end latency of **Optimal_{align}**, i.e.,*

$$\text{TEL}(\text{Sorted-F}_{\text{align}}; \mathcal{I}) \leq \text{TEL}(\text{Optimal}_{\text{align}}; \mathcal{I}).$$

Proof of Theorem 8: The key insight is that minimizing total end-to-end latency for a fixed makespan requires maximizing throughput in the earliest possible time intervals. This relationship is captured precisely by our throughput metric $\Phi(\mathcal{X}_k) = n_k / \bar{o}_k$, which measures requests completed

per unit time in batch \mathcal{X}_k . Notably, this metric is exactly the reciprocal of our quality metric $F(\mathcal{X}_k)$, establishing a direct connection between our optimization objective and scheduling efficiency.

The algorithm **Sorted-F_{align}** is designed to explicitly optimize for early throughput maximization by minimizing $F(\mathcal{X}_k)$. For each batch \mathcal{X}_k , given the fixed prior batches $\mathcal{X}_1, \mathcal{X}_2, \dots, \mathcal{X}_{k-1}$, **Sorted-F_{align}** achieves the minimal possible $F(\mathcal{X}_k)$, thereby maximizing $\Phi(\mathcal{X}_k)$.

Furthermore, the memory utilization efficiency comparison reveals a significant advantage: in Algorithm **Sorted-F_{align}**, each group \mathcal{Y}_m achieves $\eta_m \geq 1/2$ by (5), whereas in **Optimal_{align}**, the scaled allocation limits the efficiency to $\eta_{[t_g, t_{g+1}]} \leq 1/6$. This efficiency gap directly translates to a strictly smaller makespan for **Sorted-F_{align}** compared to **Optimal_{align}**.

The combination of early throughput maximization and superior makespan performance conclusively demonstrates the theorem’s validity. \square

Building upon these results, we now establish Theorem 3.

Proof of Theorem 3: Given any \mathcal{I} , we combine the guarantees from Theorems 4, 5, 6, 7, and 8 to derive the following chain of inequalities for the total end-to-end latency:

$$\begin{aligned} \text{TEL}(\text{Sorted-F}; \mathcal{I}) &\leq \text{TEL}(\text{Sorted-F}_{\text{separate}}; \mathcal{I}) < 4 \cdot \text{TEL}(\text{Sorted-F}_{\text{group}}; \mathcal{I}) \\ &< 8 \cdot \text{TEL}(\text{Sorted-F}_{\text{align}}; \mathcal{I}) \leq 8 \cdot \text{TEL}(\text{Optimal}_{\text{align}}; \mathcal{I}) \leq 48 \cdot \text{TEL}(\text{Optimal}; \mathcal{I}), \end{aligned}$$

which implies that the competitive ratio of **Sorted-F** is bounded by

$$\text{CR}(\text{Sorted-F}) < 48.$$

\square

5. Approximation Algorithm and Practical Implementation under Bad Predictions

As described in Section 3, Phase 1 of **Sorted-F** requires solving the combinatorial optimization problem $\mathcal{X}^* = \arg \min_{\mathcal{X} \subseteq \mathcal{I}} F(\mathcal{X})$ subject to the memory feasibility constraints. When this Phase 1 subproblem is solved exactly, the resulting schedule corresponds to the idealized **Sorted-F** analyzed in Section 4. However, exhaustive search is infeasible for large request sets, so we present one exact solver, such as dynamic programming, as a benchmark, and two scalable heuristics for practical use. The heuristic methods are included for empirical performance and runtime considerations; we do not claim worst-case approximation guarantees for them, nor do we claim that the constant-factor bound in Section 4 carries over when Phase 1 is implemented heuristically.

5.1. Exact Dynamic Programming

This algorithm employs dynamic programming to find the optimal request subset $\mathcal{X}^* \subseteq \mathcal{I}$ that minimizes the quality metric $F(\mathcal{X})$ within memory constraint M . The solution leverages a dual-component state representation:

$$\begin{aligned} \text{State:} \quad & dp[k][m] = \min \left\{ \sum_{r_i \in \mathcal{X}} o_i : |\mathcal{X}| = k, \sum_{r_j \in \mathcal{X}} (s_j + o_j) = m \right\} \\ \text{Path:} \quad & path[k][m] = \mathcal{X} \text{ achieving } dp[k][m] \\ \text{Objective:} \quad & \mathcal{X}^* = \arg \min_{\substack{k \in [1, n] \\ m \leq M}} \left\{ \frac{dp[k][m]}{k^2} \right\} \end{aligned}$$

The state $dp[k][m]$ captures the minimal sum of output lengths for any k -request batch consuming m memory, while the path component $path[k][m]$ records the actual request indices achieving this value. This dual representation enables efficient exploration of the solution space and exact reconstruction of the optimal request set. The complete procedure is formalized in Algorithm 2, which can be found in Appendix EC.3.

The reverse traversal order is essential to prevent multiple inclusions of the same request while preserving the optimal substructure property. Path reconstruction occurs after all state transitions complete, converting stored indices into actual request objects. The $O(n^2M)$ complexity provides a practical exact solution for moderate-scale deployments where $n \leq 100$, establishing the fundamental benchmark for Phase 1 batch selection. In particular, when Phase 1 is solved exactly, the resulting Sorted-F schedule matches the algorithmic assumption underlying the constant-factor analysis in Section 4.

5.2. Local Swap Search

This heuristic algorithm efficiently refines an initial solution through iterative local improvements. Starting with a feasible batch \mathcal{X}_0 constructed by sorting requests in ascending order of $s_i + o_i$ and applying memory-constrained greedy selection, the method systematically explores request swaps to progressively enhance solution quality. The approach exploits the combinatorial structure of the optimization landscape while avoiding exhaustive search.

The core operation is pairwise exchange: for any $r_{out} \in \mathcal{X}$ and $r_{in} \notin \mathcal{X}$ satisfying

1. Memory feasibility: $\text{mem} + (s_{in} + o_{in}) - (s_{out} + o_{out}) \leq M$,
2. Quality improvement: $F(\mathcal{X}') < F(\mathcal{X})$ with $\mathcal{X}' = (\mathcal{X} \setminus \{r_{out}\}) \cup \{r_{in}\}$.

Formally, the iterative refinement is described by

$$\mathcal{X}_{k+1} = \begin{cases} \mathcal{X}_k & \nexists \text{ improving swap} \\ \mathcal{X}_k \oplus (r_{in}, r_{out}) & F(\mathcal{X}_k \oplus (r_{in}, r_{out})) < F(\mathcal{X}_k), \end{cases}$$

where \oplus denotes the exchange operation. The algorithm terminates at local minima where no improving swaps exist. The complete procedure is formalized in Algorithm 3, which can be found in Appendix EC.3.

The $O(n^2)$ complexity enables deployment at scale $n \leq 500$. This method is a heuristic: it may get trapped in local minima and we do not provide a worst-case approximation guarantee for the Phase 1 objective. Consequently, when Phase 1 is implemented via Local Swap Search, we do not claim that the constant competitive-ratio bound proved in Section 4 continues to hold.

5.3. Quantile Greedy Selection

This approach efficiently handles large-scale scheduling problems by combining statistical sampling with two-phase greedy selection. The method strategically limits outlier requests while optimizing memory utilization for maximum throughput:

$$\begin{aligned} \text{Phase 1 (Core Selection):} & \quad \mathcal{X}_1 = \{r_i \in \mathcal{I} : s_i + o_i \leq Q_p, o_i \leq Q_o\} \\ \text{Phase 2 (Capacity Filling):} & \quad \mathcal{X} = \mathcal{X}_1 \cup \{r_j \in \mathcal{I} \setminus \mathcal{X}_1 : \text{mem} + s_j + o_j \leq M\}, \end{aligned}$$

where quantile thresholds Q_p and Q_o are derived from workload sampling. The complete pseudocode is provided in Algorithm 4 in Appendix EC.3.

The $O(n)$ complexity ensures practical deployment for large-scale systems with $n \geq 1000$ requests. This method is designed as a lightweight heuristic based on distributional trimming and greedy filling; we do not provide a worst-case approximation guarantee for the Phase 1 objective. Accordingly, when Phase 1 is implemented via Quantile Greedy Selection, we do not claim that the constant competitive-ratio bound proved in Section 4 continues to hold.

5.4. Algorithm Selection Guidelines

The three approximation algorithms present distinct operational characteristics that enable optimized deployment across the scalability spectrum. System designers should consider the algorithmic trade-offs in terms of solution quality, computational efficiency, and applicability range when selecting schedulers for specific deployment scenarios. The comparative properties are formally summarized in Table 3, which serves as the primary reference for implementation decisions.

Selection decisions should prioritize alignment between algorithm capabilities and deployment requirements. Accuracy-sensitive systems may favor the exact DP despite its computational cost,

Table 3 Algorithmic Properties and Operational Ranges (Phase 1 subproblem solvers)

Algorithm	Guarantee	Complexity	Recommended Scale
Exact Dynamic Programming	Exact optimum	$O(n^2M)$	$n \leq 100$
Local Swap Search	Heuristic	$O(n^2)$	$n \leq 500$
Quantile Greedy	Heuristic	$O(n)$	$n \geq 1000$

while latency-critical large-scale deployments benefit from linear-time heuristics. For moderate-scale systems with $200 \leq n \leq 500$, the local search approach offers a balanced compromise with quadratic complexity that remains computationally manageable. Environmental factors including workload heterogeneity and available hardware resources further influence implementation choices; heterogeneous systems may particularly benefit from the Quantile Greedy’s distribution-aware selection that helps constrain outlier impact. We emphasize that the Local Swap and Quantile Greedy procedures are included primarily for computational efficiency and observed performance; we do not provide worst-case approximation guarantees for them, nor do we claim that the constant-factor bound in Section 4 applies when Phase 1 is solved heuristically. Hybrid implementations can dynamically switch algorithms based on real-time request volume to maintain robust performance across varying load conditions. In the next section, we will compare the performance of these methods on real-data numerical experiments.

5.5. Handling Prediction Uncertainty via Adaptive Output Length Refinement

The algorithms presented thus far assume that output lengths o_i are known exactly. In practice, output lengths must be predicted, and predictions are inherently imperfect. We now describe how to extend `Sorted-F` to operate robustly under prediction uncertainty by incorporating the adaptive refinement strategy of Chen et al. (2025).

Prediction Model. For each request i , a machine learning predictor provides an interval $[\ell_i, u_i]$ such that the true output length satisfies $o_i \in [\ell_i, u_i]$. Such interval predictions arise naturally from classification-based predictors that assign requests to output-length bins. The ratio $\alpha := \inf_i \ell_i / u_i \in (0, 1]$ captures prediction confidence; smaller α indicates greater uncertainty.

Challenges with Naïve Approaches. Two straightforward strategies are to substitute o_i with either u_i (conservative) or ℓ_i (optimistic) throughout the algorithm. The conservative approach, termed \mathcal{A}_{\max} in Chen et al. (2025), prevents memory overflow but suffers from severe performance degradation as prediction accuracy decreases—memory is over-reserved, reducing throughput. The optimistic approach risks memory violations when actual output lengths exceed predictions.

Adaptive Refinement via \mathcal{A}_{\min} . The key insight of [Chen et al. \(2025\)](#) is to start optimistically and adapt during inference. Their algorithm \mathcal{A}_{\min} initially treats each request’s output length as the lower bound ℓ_i . During inference, if request i has generated \tilde{o}_i tokens without completing, its effective output length estimate is updated to \tilde{o}_i . This dynamic refinement allows the scheduler to react to actual generation progress rather than committing to potentially inaccurate predictions. When memory overflow is projected, \mathcal{A}_{\min} employs ordered eviction: requests with smaller current estimates \tilde{o}_i are removed from the active batch first, as they are closer to completion and their eviction frees memory with minimal wasted computation.

*Integration with **Sorted-F**.* We integrate adaptive refinement into **Sorted-F** as follows. In Phase 1, batch construction uses the predicted lower bounds ℓ_i in place of o_i when evaluating the objective $F(\mathcal{X})$ and checking memory feasibility. In Phase 2, the scheduling execution maintains a running estimate \tilde{o}_i for each active request, initialized to ℓ_i and updated to $\max\{\tilde{o}_i, t - p_i\}$ at each time step t , where p_i is the start time of request i . Memory feasibility checks use these running estimates. If at any time step the projected memory usage exceeds M , ordered eviction is triggered: requests are removed from the active set in increasing order of \tilde{o}_i until feasibility is restored. Evicted requests are returned to the pending queue and may be rescheduled in subsequent batches.

The combined algorithm, which we call **Sorted-F**+ \mathcal{A}_{\min} , is summarized in [Algorithm 5](#) in [Appendix EC.3](#). This integration preserves the batch construction logic of **Sorted-F** while inheriting the robustness properties of \mathcal{A}_{\min} for handling prediction errors.

6. Extensions and Discussions

Building on our earlier work—where we proposed the **Sorted-F** algorithm and established its constant-factor competitive ratio for this NP-hard problem—we now discuss alternative formulations and heuristics based on integer programming (IP) and linear programming (LP). The goal of this section is twofold: (i) to use IP/LP to further illuminate the structure of the problem (e.g., via relaxations and lower bounds), and (ii) to derive practical LP-guided scheduling heuristics that serve as complementary baselines in our numerical evaluation. We emphasize that the LP-based methods below, **Sorted-LP** and **LP-Swap**, are heuristics: we do not provide worst-case approximation/competitive-ratio guarantees for their rounded schedules, and the integrality gap of the relaxation is not characterized here.

From [Jaillet et al. \(2025\)](#), the offline optimum can be formulated as the following integer program:

$$\text{Optimal-IP} = \min \sum_{i \in [n]} \left(\sum_{t=\{0, \dots, \bar{T}\}} t \cdot x_{i,t} + o_i \right) \quad (7)$$

$$\text{s.t. } \sum_{t=\{0,\dots,\bar{T}\}} x_{i,t} = 1, \quad \forall i \in [n] \quad (8)$$

$$\sum_{i=1}^n \sum_{k=\max\{0,t-o_i\}}^{t-1} (s_i + t - k)x_{i,k} \leq M, \quad \forall t \in [\bar{T}] \quad (9)$$

$$x_{i,t} \in \{0, 1\}, \quad \forall i \in [n], \forall t \in [\bar{T}] \quad (10)$$

where \bar{T} is an upper bound on the time horizon. The decision variables are $x_{i,t}$. If $x_{i,t} = 1$, request i starts at time t . Constraint (8) enforces that each request starts exactly once, and constraint (9) ensures that at any time t , the total KV-cache memory usage does not exceed M .

Since solving Optimal-IP is computationally intractable, we relax the integrality constraints and obtain the following LP:

$$\text{Relaxed-LP} = \min \sum_{i \in [n]} \left(\sum_{t=\{0,\dots,\bar{T}\}} t \cdot x_{i,t} + o_i \right) \quad (11)$$

$$\text{s.t. } \sum_{t=\{0,\dots,\bar{T}\}} x_{i,t} = 1, \quad \forall i \in [n] \quad (12)$$

$$\sum_{i=1}^n \sum_{k=\max\{0,t-o_i\}}^{t-1} (s_i + t - k)x_{i,k} \leq M, \quad \forall t \in [\bar{T}] \quad (13)$$

$$x_{i,t} \geq 0. \quad \forall i \in [n], \forall t \in [\bar{T}] \quad (14)$$

The Relaxed-LP objective value provides a valid lower bound on Optimal-IP and thus on the offline optimal latency. However, optimal LP solutions $x_{i,t}^*$ are typically fractional, and converting them into a feasible discrete schedule requires rounding or other heuristics. In what follows, we introduce two LP-guided scheduling heuristics, **Sorted-LP** and **LP-Swap**, whose effectiveness is assessed empirically (Appendix EC.4.2 and Section 7). We do not claim provable guarantees for these rounded schedules; in particular, the integrality gap of Relaxed-LP and the approximation quality of the rounding procedures are left for future work.

Sorted-LP: LP-induced ordering heuristic. The algorithm proceeds in three steps. First, it solves Relaxed-LP to obtain an optimal fractional solution $x_{i,t}^*$. Second, for each request i , it computes the LP-induced average expected start time

$$y_i = \sum_{t \in [\bar{T}]} t \cdot x_{i,t}^*.$$

Finally, **Sorted-LP** sorts requests by increasing y_i and then executes them using the same feasible admission rule as in Phase 2 of **Sorted-F**. Intuitively, smaller y_i indicates that the LP relaxation “prefers” starting request i earlier; we use this as an ordering signal rather than a guarantee. The detailed procedure is formalized in Algorithm 6 in Appendix EC.4.1.

LP-Swap: LP ordering + F-metric refinement. While **Sorted-LP** provides a principled ordering signal from the LP relaxation, it may be further improved by incorporating our F-metric framework. To this end, we propose **LP-Swap**, a hybrid approach that starts from the **Sorted-LP**-induced ordering and then applies F-metric-guided local swap refinements when forming batches. This hybrid strategy leverages both the global perspective captured by the LP relaxation and the local optimization capability of the swap procedure. The complete pseudocode is provided in Algorithm 7 in Appendix EC.4.1. We evaluate the effectiveness of these LP-based heuristics using simulated data in Appendix EC.4.2 and compare them on the real dataset in Section 7.

7. Numerical Experiments

In this section, we conduct a numerical experiment with open-source real datasets to evaluate the performance of **Sorted-F** and its approximations, including the newly proposed **Sorted-LP** and **LP-Swap**.

Dataset Overview. To evaluate LLM inference performance under varying input prompt lengths—particularly in scenarios mixing short and long prompts—we combine two publicly available datasets, as no single existing dataset meets this need. The first dataset, introduced by Zheng et al. (2023a), contains conversational data from over 210,000 unique IP addresses, collected via the Vicuna demo and Chatbot Arena. This dataset, available at <https://huggingface.co/datasets/lmsys/lmsys-chat-1m>, consists of short, interactive exchanges with a mean input length of 41.84 tokens (median: 12.00) and a mean output length of 85.35 tokens (median: 43.00), as shown in Figure 6.

The second dataset, constructed by Cohan et al. (2018), focuses on long-form summarization of academic papers from Arxiv (available at <https://github.com/armancohan/long-summarization>). Here, prompts are significantly longer, with a mean input length of 2546.39 tokens (median: 2667.50) and a mean output length of 296.08 tokens (median: 161.00), illustrated in Figure 6.

From these datasets, we randomly select 1600 short conversations and 400 long summarization tasks. By merging them with a random permutation, we create a mixed dataset of 2000 samples. Figure 7 reveals the resulting distribution: the input lengths now exhibit a mean of 542.75 tokens (median: 18.00), while outputs have a mean of 127.50 tokens, demonstrating the desired variability in prompt sizes.

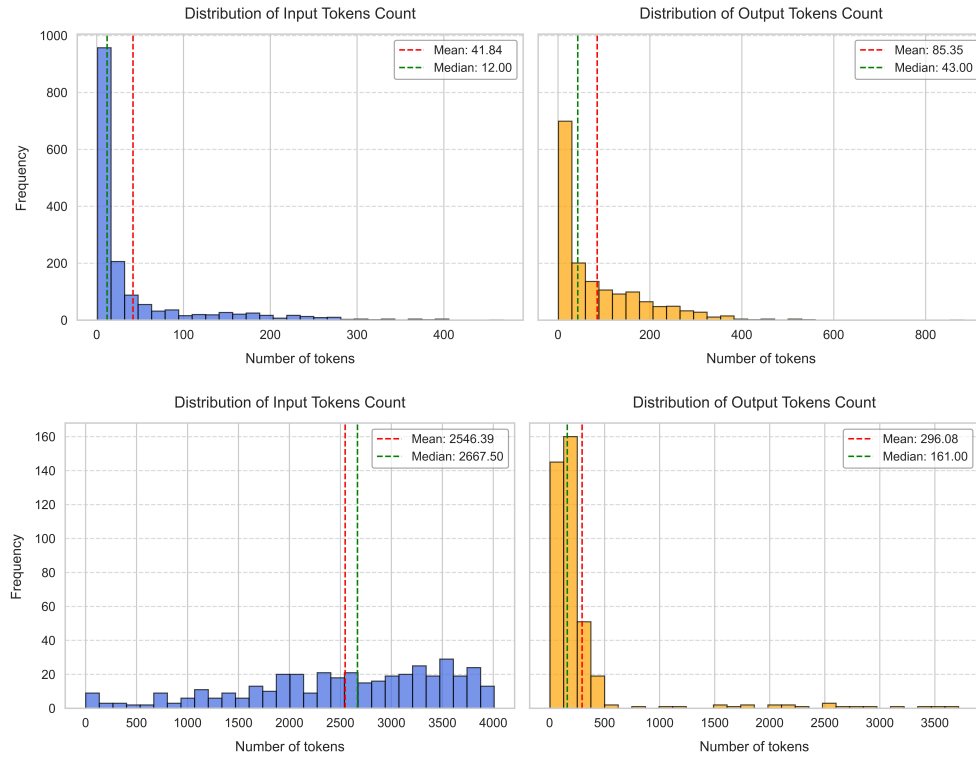


Figure 6 Upper: Distribution of the number of tokens of input prompt and output response respectively in the data [Zheng et al. \(2023a\)](#). Lower: Distribution of the number of tokens of input prompt and output response respectively in the data [Cohan et al. \(2018\)](#).

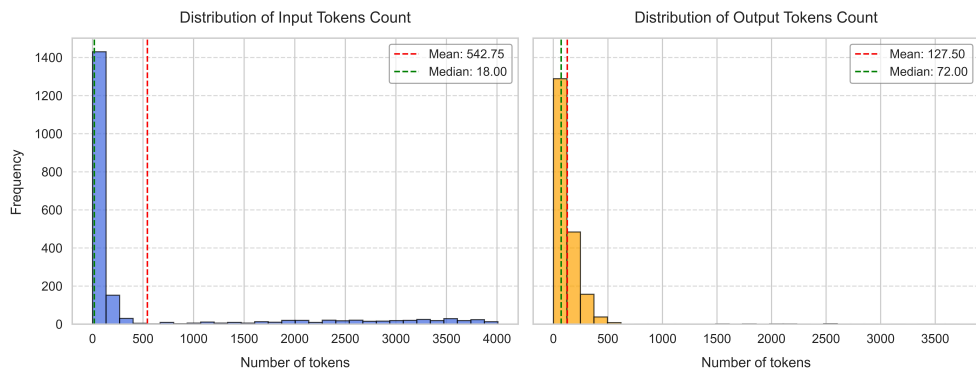


Figure 7 Distribution of the number of tokens of input prompt and output response respectively in the mixed data

Experiment Setup. We evaluate performance using averaged end-to-end latency, defined as the total latency across all requests divided by the number of requests. For benchmarking, we compare against three algorithms:

1. **FCFS**: Requests are processed in the order they arrive (determined by random shuffling of the mixed dataset). Each batch is filled maximally without exceeding memory limits, assuming perfect knowledge of output lengths.
2. **MC-SF**: As described in Section 2.3, this strategy prioritizes requests with shorter output lengths to minimize batch processing time.
3. **Sorted-LP**: Introduced in Section 6, **Sorted-LP** solves a relaxed linear program to estimate request starting times, then batches requests in ascending order of these values.
4. **LP-Swap**: The hybrid method outlined in Section 6, combining **Sorted-LP** ordering with F-metric-guided swaps.

To test our proposed algorithm, **Sorted-F**, we face computational constraints: exact dynamic programming is intractable for 2000 requests. Instead, we employ the local swap search and the quantile greedy selection approximation methods.

For scalability analysis, we evaluate latency trends by subsampling the mixed dataset (200, 400, ..., 2000 requests). All simulations emulate deployment of LLaMA2-70B on two A100 GPUs, with a KV cache memory limit of 16,492 tokens. Batch processing times are estimated using the linear regression method in the Vidur simulator from Agrawal et al. (2024a).

Results. Figure 8 compares the averaged latency across scheduling algorithms, revealing key insights.

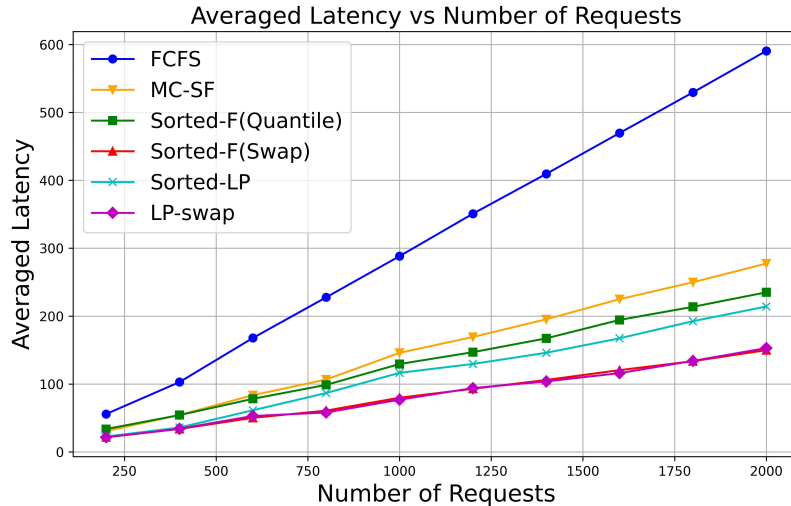


Figure 8 Averaged latency between different scheduling algorithms

First, the inferior performance of **MC-SF** relative to **Sorted-F** and **Sorted-LP** underscores the importance of accounting for variable input sizes—purely output-length-based prioritization (**MC-SF**) proves inadequate for mixed workloads.

For our proposed **Sorted-F** algorithm, the results align with the theoretical analysis in Section 5: the quantile greedy selection achieves faster runtime, while the local swap method delivers superior latency performance. This trade-off highlights the practical value of both approximation approaches.

Notably, **LP-Swap** demonstrates significant latency reduction over its base algorithm **Sorted-LP**, validating that incorporating the F-metric substantially improves LP-based schedules. However, the performance of **LP-Swap** achieves nearly identical latency to **Sorted-F** (Swap), as demonstrated in the detailed comparison provided in Appendix EC.5 (Figure EC.2). This indicates that the initial LP-based ordering provides no unique advantage over direct F-metric optimization, as both converge to similar schedules after swap refinement. This empirically confirms that F-metric-guided optimization is highly effective irrespective of initial scheduling. The robustness of the F-metric as a scheduling criterion is thus reinforced, and **Sorted-F** remains highly competitive due to its significantly faster computation time and simpler implementation.

References

- Amey Agrawal, Nitin Kedia, Jayashree Mohan, Ashish Panwar, Nipun Kwatra, Bhargav Gulavani, Ramachandran Ramjee, and Alexey Tumanov. 2024a. Vidur: A Large-Scale Simulation Framework For LLM Inference. *Proceedings of Machine Learning and Systems* 6 (2024), 351–366.
- Amey Agrawal, Nitin Kedia, Ashish Panwar, Jayashree Mohan, Nipun Kwatra, Bhargav S Gulavani, Alexey Tumanov, and Ramachandran Ramjee. 2024b. Taming throughput-latency tradeoff in LLM inference with Sarathi-Serve. *arXiv preprint arXiv:2403.02310* (2024).
- Amey Agrawal, Ashish Panwar, Jayashree Mohan, Nipun Kwatra, Bhargav S Gulavani, and Ramachandran Ramjee. 2023. Sarathi: Efficient LLM inference by piggybacking decodes with chunked prefills. *arXiv preprint arXiv:2308.16369* (2023).
- Kunal Agrawal, Jing Li, Kefu Lu, and Benjamin Moseley. 2016. Scheduling parallel DAG jobs online to minimize average flow time. In *Proceedings of the Twenty-Seventh Annual ACM-SIAM Symposium on Discrete Algorithms* (Arlington, Virginia) (*SODA '16*). Society for Industrial and Applied Mathematics, USA, 176–189.
- Susanne Albers. 2009. Online scheduling. In *Introduction to scheduling*. CRC Press, 71–98.
- Ali Allahverdi, Chi To Ng, TC Edwin Cheng, and Mikhail Y Kovalyov. 2008. A survey of scheduling problems with setup times or costs. *European journal of operational research* 187, 3 (2008), 985–1032.

- Amazon. 2023. Amazon CodeWhisperer. <https://aws.amazon.com/codewhisperer/>.
- Anthropic. 2023. Claude. <https://claude.ai>.
- Ruicheng Ao, Gan Luo, David Simchi-Levi, and Xinshang Wang. 2025. Optimizing LLM Inference: Fluid-Guided Online Scheduling with Memory Constraints. *arXiv preprint arXiv:2504.11320* (2025).
- Yossi Azar and Leah Epstein. 2002. On-line scheduling with precedence constraints. *Discrete Applied Mathematics* 119, 1 (2002), 169–180. [https://doi.org/10.1016/S0166-218X\(01\)00272-4](https://doi.org/10.1016/S0166-218X(01)00272-4) Special Issue devoted to Foundation of Heuristics in Combinatoria I Optimization.
- Tom Brown, Benjamin Mann, Nick Ryder, Melanie Subbiah, Jared D Kaplan, Prafulla Dhariwal, Arvind Neelakantan, Pranav Shyam, Girish Sastry, Amanda Askell, et al. 2020. Language models are few-shot learners. *Advances in neural information processing systems* 33 (2020), 1877–1901.
- Peter Brucker, Andreas Drexler, Rolf Möhring, Klaus Neumann, and Erwin Pesch. 1999. Resource-constrained project scheduling: Notation, classification, models, and methods. *European journal of operational research* 112, 1 (1999), 3–41.
- Peter Brucker, Andrei Gladky, Han Hoogeveen, Mikhail Y Kovalyov, Chris N Potts, Thomas Tautenhahn, and Steef L Van De Velde. 1998. Scheduling a batching machine. *Journal of scheduling* 1, 1 (1998), 31–54.
- Marco Cascella, Jonathan Montomoli, Valentina Bellini, and Elena Bignami. 2023. Evaluating the feasibility of ChatGPT in healthcare: an analysis of multiple clinical and research scenarios. *Journal of medical systems* 47, 1 (2023), 33.
- Bo Chen and Chung-Yee Lee. 2008. Logistics scheduling with batching and transportation. *European journal of operational research* 189, 3 (2008), 871–876.
- Bo Chen, Chris N Potts, and Gerhard J Woeginger. 1998. A review of machine scheduling: Complexity, algorithms and approximability. *Handbook of Combinatorial Optimization: Volume1–3* (1998), 1493–1641.
- Shiyang Chen, Rain Jiang, Dezhi Yu, Jinlai Xu, Mengyuan Chao, Fanlong Meng, Chenyu Jiang, Wei Xu, and Hang Liu. 2024. KVDirect: Distributed Disaggregated LLM Inference. *arXiv preprint arXiv:2501.14743* (2024).
- Zixi Chen, Tianci Bu, Chendong Song, Xin Lu, Yinyu Ye, and Zijie Zhou. 2026. A Universal Load Balancing Principle and Its Application to Large Language Model Serving. *arXiv preprint arXiv:2601.17855* (2026).
- Zixi Chen, Yinyu Ye, and Zijie Zhou. 2025. Adaptively robust llm inference optimization under prediction uncertainty. *arXiv preprint arXiv:2508.14544* (2025).
- Aakanksha Chowdhery, Sharan Narang, Jacob Devlin, Maarten Bosma, Gaurav Mishra, Adam Roberts, Paul Barham, Hyung Won Chung, Charles Sutton, Sebastian Gehrmann, et al. 2023. Palm: Scaling language modeling with pathways. *Journal of Machine Learning Research* 24, 240 (2023), 1–113.

-
- Arman Cohan, Franck Deroncourt, Doo Soon Kim, Trung Bui, Seokhwan Kim, Walter Chang, and Nazli Goharian. 2018. A discourse-aware attention model for abstractive summarization of long documents. *arXiv preprint arXiv:1804.05685* (2018).
- Yichao Fu, Siqi Zhu, Runlong Su, Aurick Qiao, Ion Stoica, and Hao Zhang. 2024. Efficient LLM Scheduling by Learning to Rank. *arXiv preprint arXiv:2408.15792* (2024).
- Naveen Garg, Anupam Gupta, Amit Kumar, and Sahil Singla. 2019. Non-Clairvoyant Precedence Constrained Scheduling. In *46th International Colloquium on Automata, Languages, and Programming, ICALP 2019, July 9-12, 2019, Patras, Greece (LIPIcs, Vol. 132)*, Christel Baier, Ioannis Chatzigiannakis, Paola Flocchini, and Stefano Leonardi (Eds.). Schloss Dagstuhl - Leibniz-Zentrum für Informatik, 63:1–63:14. <https://doi.org/10.4230/LIPICSLP.2019.63>
- GitHub. 2021. GitHub Copilot. <https://github.com/features/copilot>.
- Google. 2023. Bard. <https://bard.google.com>.
- Patrick Jaillet, Jiashuo Jiang, Konstantina Mellou, Marco Molinaro, Chara Podimata, and Zijie Zhou. 2025. Online Scheduling for LLM Inference with KV Cache Constraints. *arXiv preprint arXiv:2502.07115* (2025).
- Qingxia Kong, Chung-Yee Lee, Chung-Piaw Teo, and Zhichao Zheng. 2013. Scheduling arrivals to a stochastic service delivery system using copositive cones. *Operations research* 61, 3 (2013), 711–726.
- Woosuk Kwon, Zhuohan Li, Siyuan Zhuang, Ying Sheng, Lianmin Zheng, Cody Hao Yu, Joseph Gonzalez, Hao Zhang, and Ion Stoica. 2023. Efficient memory management for large language model serving with PagedAttention. In *Proceedings of the 29th Symposium on Operating Systems Principles*. 611–626.
- Wenhua Li, Libo Wang, Xing Chai, and Hang Yuan. 2020. Online batch scheduling of simple linear deteriorating jobs with incompatible families. *Mathematics* 8, 2 (2020), 170.
- Yueying Li, Jim Dai, and Tianyi Peng. 2025. Throughput-optimal scheduling algorithms for llm inference and ai agents. *arXiv preprint arXiv:2504.07347* (2025).
- Peihai Liu and Xiwen Lu. 2015. Online unbounded batch scheduling on parallel machines with delivery times. *Journal of Combinatorial Optimization* 29 (2015), 228–236.
- Ho-Yin Mak, Ying Rong, and Jiawei Zhang. 2015. Appointment scheduling with limited distributional information. *Management Science* 61, 2 (2015), 316–334.
- Microsoft. 2023. Bing AI. <https://www.bing.com/chat>.
- OpenAI. 2023. GPT-4 technical report. arxiv 2303.08774. *View in Article* 2, 5 (2023).
- Pratyush Patel, Esha Choukse, Chaojie Zhang, Aashaka Shah, Íñigo Goiri, Saeed Maleki, and Ricardo Bianchini. 2023. Splitwise: Efficient generative LLM inference using phase splitting. *Power* 400, 700W (2023), 1–75.

- Cheng Peng, Xi Yang, Aokun Chen, Kaleb E Smith, Nima PourNejatian, Anthony B Costa, Cheryl Martin, Mona G Flores, Ying Zhang, Tanja Magoc, et al. 2023. A study of generative large language model for medical research and healthcare. *NPJ digital medicine* 6, 1 (2023), 210.
- Haoran Qiu, Weichao Mao, Archit Patke, Shengkun Cui, Saurabh Jha, Chen Wang, Hubertus Franke, Zbigniew T Kalbarczyk, Tamer Başar, and Ravishankar K Iyer. 2024. Efficient interactive LLM serving with proxy model-based sequence length prediction. *arXiv preprint arXiv:2404.08509* (2024).
- Julien Robert and Nicolas Schabanel. 2008. Non-clairvoyant scheduling with precedence constraints. In *Proceedings of the Nineteenth Annual ACM-SIAM Symposium on Discrete Algorithms, SODA 2008, San Francisco, California, USA, January 20-22, 2008*, Shang-Hua Teng (Ed.). SIAM, 491–500. <http://dl.acm.org/citation.cfm?id=1347082.1347136>
- Rana Shahout, Eran Malach, Chunwei Liu, Weifan Jiang, Minlan Yu, and Michael Mitzenmacher. 2024. Don't Stop Me Now: Embedding Based Scheduling for LLMs. *arXiv preprint arXiv:2410.01035* (2024).
- Ashish Vaswani, Noam Shazeer, Niki Parmar, Jakob Uszkoreit, Llion Jones, Aidan N Gomez, Lukasz Kaiser, and Illia Polosukhin. 2017. Attention is all you need. *Advances in neural information processing systems* 30 (2017).
- Wenxun Xing and Jiawei Zhang. 2000. Parallel machine scheduling with splitting jobs. *Discrete Applied Mathematics* 103, 1-3 (2000), 259–269.
- Gyeong-In Yu, Joo Seong Jeong, Geon-Woo Kim, Soojeong Kim, and Byung-Gon Chun. 2022. Orca: A distributed serving system for {Transformer-Based} generative models. In *16th USENIX Symposium on Operating Systems Design and Implementation (OSDI 22)*. 521–538.
- Lianmin Zheng, Wei-Lin Chiang, Ying Sheng, Tianle Li, Siyuan Zhuang, Zhanghao Wu, Yonghao Zhuang, Zhuohan Li, Zi Lin, Eric Xing, et al. 2023a. LMSYS-Chat-1M: A large-scale real-world LLM conversation dataset. *arXiv preprint arXiv:2309.11998* (2023).
- Zangwei Zheng, Xiaozhe Ren, Fuzhao Xue, Yang Luo, Xin Jiang, and Yang You. 2023b. Response length perception and sequence scheduling: An llm-empowered llm inference pipeline. *Advances in Neural Information Processing Systems* 36 (2023), 65517–65530.
- Yinmin Zhong, Shengyu Liu, Junda Chen, Jianbo Hu, Yibo Zhu, Xuanzhe Liu, Xin Jin, and Hao Zhang. 2024. Distserve: Disaggregating prefill and decoding for goodput-optimized large language model serving. *arXiv preprint arXiv:2401.09670* (2024).

Appendix: Proofs of Statements

EC.1. Supplementary Materials for Section 2

Proof of Theorem 1: Consider the following instance \mathcal{I} with two types of requests:

- Type 1: each request has size $s = \sqrt{M} - 1$, output length $o = 1$, and there are $X = M$ such requests.
- Type 2: each request has size $s = 1$, output length $o = 2$, and there are $Y = M^{1.25}$ such requests.

Under MC-SF, which processes all type 1 requests before any type 2 request (since type 1 requests are shorter), the total expected latency is

$$\text{TEL}(\text{MC-SF}; \mathcal{I}) = \sqrt{M} \sum_{i=1}^{X/\sqrt{M}} i + \frac{XY}{\sqrt{M}} + \frac{2M}{3} \sum_{j=1}^{3Y/M} j.$$

Now consider an alternative schedule Λ that processes all type 2 requests before any type 1 request. Its total latency is

$$\text{TEL}(\Lambda; \mathcal{I}) = \frac{2M}{3} \sum_{j=1}^{3Y/M} j + \frac{6XY}{M} + \sqrt{M} \sum_{i=1}^{X/\sqrt{M}} i.$$

We compare the two total latencies:

$$\frac{\text{TEL}(\text{MC-SF}; \mathcal{I})}{\text{TEL}(\Lambda; \mathcal{I})} = \frac{M^{1.75} + \frac{7}{2}M^{1.5} + M^{1.25} + \frac{1}{2}M}{\frac{7}{2}M^{1.5} + 7M^{1.25} + \frac{1}{2}M} \geq \frac{1}{11}M^{0.25}.$$

Hence, the competitive ratio of MC-SF grows unboundedly as $M \rightarrow \infty$, implying that $\text{CR}(\text{MC-SF}) \rightarrow \infty$. \square

THEOREM EC.1. *Suppose that each request $i \in [n]$ satisfies $s_i \in [1, M]$, $o_i \in [1, M]$ and $s_i + o_i \leq M$, then Algorithm MC-SF₂ (process the smallest $s_i + o_i$ first) achieves an unbounded competitive ratio. Specifically, as $M \rightarrow \infty$, we have*

$$\text{CR}(\text{MC-SF}_2) \rightarrow \infty.$$

Proof of Theorem EC.1: Consider the following instance \mathcal{I} with two types of requests:

- Type 1: each request has size $s = 1$, output length $o = \sqrt{M} - 1$, and there are $X = M$ such requests.
- Type 2: each request has size $s = \sqrt{M}$, output length $o = 1$, and there are $Y = M^{1.5}$ such requests.

Under MC-SF₂, which processes all type 1 requests before any type 2 request (since type 1 requests are shorter), the total expected latency is

$$\text{TEL}(\text{MC-SF}_2; \mathcal{I}) = (\sqrt{M} - 1)\sqrt{M} \sum_{i=1}^{X/\sqrt{M}} i + (\sqrt{M} - 1) \frac{XY}{\sqrt{M}} + \sqrt{M} \sum_{j=1}^{Y/\sqrt{M}} j.$$

Now consider an alternative schedule \mathcal{A} that processes all type 2 requests before any type 1 request. Its total latency is

$$\text{TEL}(\mathcal{A}; \mathcal{I}) = (\sqrt{M} - 1)\sqrt{M} \sum_{i=1}^{X/\sqrt{M}} i + \frac{XY}{\sqrt{M}} + \sqrt{M} \sum_{j=1}^{Y/\sqrt{M}} j.$$

We compare the two total latencies:

$$\frac{\text{TEL}(\text{MC-SF}_2; \mathcal{I})}{\text{TEL}(\mathcal{A}; \mathcal{I})} = \frac{\frac{1}{2}M^2 + M^{2.5} + \frac{1}{2}M^{1.75}}{\frac{1}{2}M^2 + M^2 + \frac{1}{2}M^{1.75}} \geq \frac{2}{3}M^{0.5}.$$

Hence, the competitive ratio of MC-SF₂ grows unboundedly as $M \rightarrow \infty$, implying that $\text{CR}(\text{MC-SF}_2) \rightarrow \infty$. \square

Proof of Theorem 2 We prove this via a reduction from the 3-Partition problem, which is known to be strongly NP-hard. Consider the following 3-Partition Problem: Given a multiset of integers $X = \{x_1, \dots, x_{3m}\}$ summing to mT , where each x_i satisfies $T/4 < x_i < T/2$, the problem asks whether X can be partitioned into m disjoint subsets S_1, \dots, S_m such that the sum of each subset equals T .

Then, we construct the following reduction: Given an instance of 3-Partition, we construct an instance as follows:

- For each integer x_i , create a request i with $s_i = x_i$ and $o_i = 1$.
- Set the memory capacity $M = T$.

We show that the 3-Partition instance has a solution if and only if the constructed instance has a schedule with total end-to-end latency $\text{TEL} = \frac{3m(m+1)}{2}$.

Case 1: 3-Partition Exists. Suppose X can be partitioned into m subsets S_1, \dots, S_m , each summing to T . Then, consider the schedule which processes batch k with all requests in S_k . The schedule is feasible since the memory usage of each batch is M . Moreover, as each batch processes exactly 3 requests (due to $T/4 < x_i < T/2$), the total end-to-end latency is

$$\text{TEL} = \sum_{t=1}^m 3t = \frac{3m(m+1)}{2}.$$

Case 2: No 3-Partition Exists. If no such partition exists, then at least one batch must process fewer than 3 requests (since no subset of 2 requests sums to $\leq T$, given $x_i > T/4$). This forces the

schedule to use at least $m + 1$ batches. Compared to the schedule in case 1, there is at least one job having to be swapped from one of the batch 1 to batch m to the batch $m + 1$, and the total end-to-end latency in this case is strictly greater than $\frac{3m(m+1)}{2}$.

Since the minimal total end-to-end latency is $\frac{3m(m+1)}{2}$ if and only if the 3-Partition instance has a solution, the problem of minimizing total end-to-end latency is NP-hard. \square

EC.2. Supplementary Materials for Section 4

Proof of Lemma 2: According to the construction of \mathcal{Y}_m , for any $k \in \{b_{m-1} + 1, b_{m-1} + 2, \dots, b_m - 1\}$, the following inequality holds:

$$\frac{\sum_{j=1}^{n_k} o_{k,j} + o_{k+1,1}}{(n_k + 1)^2} > \frac{\sum_{j=1}^{n_k} o_{k,j}}{n_k^2}.$$

This inequality implies that incorporating request $r_{k+1,1}$ into batch \mathcal{X}_k would not yield improvement in the objective function value $F(\mathcal{X}_k)$. Consequently, while such addition may remain within the memory constraint M , it is excluded by the optimality criteria of the batching procedure.

Let q_{k+1} denote the maximum number of requests from batch $k + 1$ that can be added to \mathcal{X}_k without exceeding M , i.e., $\mathcal{X}_k + [r_{k+1,1}, \dots, r_{k+1,q_{k+1}}]$ remains feasible. The critical inequality

$$\frac{\sum_{i=1}^{n_k} o_{k,i} + \sum_{j=1}^{q_{k+1}} o_{k+1,j}}{(n_k + q_{k+1})^2} > \frac{\sum_{i=1}^{n_k} o_{k,i}}{n_k^2}$$

must hold. Otherwise, incorporating these q_{k+1} requests would have improved \mathcal{X}_k by either reducing $F(\mathcal{X}_k)$ or increasing its batch size while maintaining $F(\mathcal{X}_k)$, which would contradict the optimal selection criterion of **Sorted-F**.

This inequality directly implies the following relationship between the average processing times:

$$\frac{\sum_{j=1}^{q_{k+1}} o_{k+1,j}}{q_{k+1}} > \left(2 + \frac{q_{k+1}}{n_k}\right) \cdot \frac{\sum_{i=1}^{n_k} o_{k,i}}{n_k}. \quad (\text{EC.1})$$

Next, we examine the relationship between the longest processing times $o_{k+1,n_{k+1}}$ in batch \mathcal{X}_{k+1} and o_{k,n_k} in batch \mathcal{X}_k . Since $o_{k+1,n_{k+1}}$ is the maximum processing time in \mathcal{X}_{k+1} , it dominates both individual terms and their average:

$$o_{k+1,n_{k+1}} \geq o_{k+1,q_{k+1}} \geq \frac{1}{q_{k+1}} \sum_{j=1}^{q_{k+1}} o_{k+1,j}. \quad (\text{EC.2})$$

Furthermore, Lemma 1 establishes that for large n_k , the average processing time in \mathcal{X}_k satisfies

$$\frac{1}{n_k} \sum_{i=1}^{n_k} o_{k,i} > \frac{1}{2} \cdot o_{k,n_k}.$$

Combining these results with Inequality (EC.1) yields the key relationship:

$$o_{k+1,n_{k+1}} \geq \frac{1}{q_{k+1}} \sum_{j=1}^{q_{k+1}} o_{k+1,j} > \left(2 + \frac{q_{k+1}}{n_k}\right) \cdot \frac{1}{n_k} \sum_{i=1}^{n_k} o_{k,i} > \left(2 + \frac{q_{k+1}}{n_k}\right) \cdot \frac{1}{2} o_{k,n_k} > o_{k,n_k}. \quad (\text{EC.3})$$

Subsequently, we extend the analysis to consecutive batches \mathcal{X}_{k+1} and \mathcal{X}_{k+2} for any $k \in \{b_{m-1} + 1, \dots, b_m - 2\}$. The construction similarly satisfies

$$\frac{\sum_{j=1}^{n_{k+1}} o_{k+1,j} + o_{k+2,1}}{(n_{k+1} + 1)^2} > \frac{\sum_{j=1}^{n_{k+1}} o_{k+1,j}}{n_{k+1}^2},$$

which demonstrates that including request $r_{k+2,1}$ in \mathcal{X}_{k+1} would not reduce the objective function value $F(\mathcal{X}_{k+1})$. While such inclusion may not exceed memory M , it is precluded by the optimality criteria of the batching procedure.

Let q_{k+2} denote the maximum number of requests from \mathcal{X}_{k+2} that can be added to \mathcal{X}_{k+1} without violating M . This yields two key inequalities:

$$\begin{aligned} \frac{\sum_{j=1}^{q_{k+2}} o_{k+2,j}}{q_{k+2}} &> \left(2 + \frac{q_{k+2}}{n_{k+1}}\right) \cdot \frac{\sum_{i=1}^{n_{k+1}} o_{k+1,i}}{n_{k+1}} \\ o_{k+2,n_{k+2}} &\geq o_{k+2,q_{k+2}} \geq \frac{\sum_{j=1}^{q_{k+2}} o_{k+2,j}}{q_{k+2}}. \end{aligned}$$

Furthermore, the increasing response length property implies

$$\frac{\sum_{i=1}^{n_{k+1}} o_{k+1,i}}{n_{k+1}} \geq \frac{\sum_{j=1}^{q_{k+1}} o_{k+1,j}}{q_{k+1}}.$$

Combining these results with previous Inequalities (EC.1), (EC.2), we can derive the cumulative relationship:

$$\begin{aligned} o_{k+2,n_{k+2}} &\geq \frac{\sum_{l=1}^{q_{k+2}} o_{k+2,l}}{q_{k+2}} > \left(2 + \frac{q_{k+2}}{n_{k+1}}\right) \cdot \frac{\sum_{i=1}^{n_{k+1}} o_{k+1,i}}{n_{k+1}} \geq \left(2 + \frac{q_{k+2}}{n_{k+1}}\right) \cdot \frac{\sum_{j=1}^{q_{k+1}} o_{k+1,j}}{q_{k+1}} \\ &\geq \left(2 + \frac{q_{k+2}}{n_{k+1}}\right) \cdot \left(2 + \frac{q_{k+1}}{n_k}\right) \cdot \frac{\sum_{i=1}^{n_k} o_{k,i}}{n_k} > 4 \cdot \frac{1}{2} o_{k,n_k} \\ &= 2o_{k,n_k}. \end{aligned} \quad (\text{EC.4})$$

Based on Inequalities (EC.3) and (EC.4), for any $i \in \{1, \dots, a_m\}$, we can derive the following geometric bound for all batch indices $i \in \{1, \dots, a_m\}$:

$$o_{k+i,n_{k+i}} \leq \left(\frac{1}{2}\right)^{\lfloor \frac{a-i}{2} \rfloor} \cdot o_{k+a,n_{k+a}}.$$

□

Proof of Lemma 3

$$\begin{aligned}
\text{TEL}(\text{Sorted-F}_{\text{group}}; \mathcal{I}) &= \sum_{m=1}^{\infty} \left(o_{b_m, n_{b_m}} \cdot \sum_{k=b_m+1}^{\infty} n_k \right) + \sum_{k=1}^{\infty} \sum_{i=1}^{n_k} o_{k,i} \\
&\geq \sum_{m=1}^{\infty} \left(\frac{1}{4} \cdot \sum_{l=b_{m-1}+1}^{b_m} o_{l, n_l} \cdot \sum_{k=b_m+1}^{\infty} n_k \right) + \sum_{k=1}^{\infty} \sum_{i=1}^{n_k} o_{k,i} \\
&= \frac{1}{4} \cdot \sum_{m=1}^{\infty} \left(\sum_{l=b_{m-1}+1}^{b_m} o_{l, n_l} \cdot \left(\sum_{k=b_m+1}^{\infty} n_k + o \left(\sum_{k=b_m+1}^{\infty} n_k \right) \right) \right) + \sum_{k=1}^{\infty} \sum_{i=1}^{n_k} o_{k,i} \\
&= \frac{1}{4} \cdot \sum_{m=1}^{\infty} \left(\sum_{l=b_{m-1}+1}^{b_m} o_{l, n_l} \cdot \left(\sum_{k=b_m+1}^{\infty} n_k + \sum_{k=b_{m-1}+1}^{b_m} n_k \right) \right) + \sum_{k=1}^{\infty} \sum_{i=1}^{n_k} o_{k,i} \\
&> \frac{1}{4} \cdot \sum_{m=1}^{\infty} \left(\sum_{l=b_{m-1}+1}^{b_m} o_{l, n_l} \cdot \sum_{k=b_m+1}^{\infty} n_k + \sum_{l=b_{m-1}+1}^{b_m-1} (o_{l, n_l} \cdot (b_m - l)) \right) + \sum_{k=1}^{\infty} \sum_{i=1}^{n_k} o_{k,i} \\
&> \frac{1}{4} \cdot \left(\sum_{m=1}^{\infty} \left(\sum_{l=b_{m-1}+1}^{b_m} o_{l, n_l} \cdot \sum_{k=b_m+1}^{\infty} n_k + \sum_{l=b_{m-1}+1}^{b_m-1} (o_{l, n_l} \cdot (b_m - l)) \right) + \sum_{k=1}^{\infty} \sum_{i=1}^{n_k} o_{k,i} \right) \\
&= \frac{1}{4} \cdot \text{TEL}(\text{Sorted-F}_{\text{separate}}; \mathcal{I}).
\end{aligned}$$

□

Proof of Lemma 4:

$$\begin{aligned}
\text{TEL}(\text{Optimal}_{\text{align}}; \mathcal{I}) &= \sum_{h=1}^{\infty} \left(\bar{o}_h \cdot \sum_{j=h+1}^{\infty} n_j \right) + \sum_{h=1}^{\infty} \sum_{i=1}^{n_h} o_{h,i} \\
&= \sum_{g=1}^{\infty} \sum_{h=d_{g-1}+1}^{d_g} \left(\bar{o}_h \cdot \left(\sum_{j=h+1}^{d_g} n_j + \sum_{j=d_g+1}^{\infty} n_j \right) \right) + \sum_{h=1}^{\infty} \sum_{i=1}^{n_h} o_{h,i} \\
&= \sum_{g=1}^{\infty} \sum_{h=d_{g-1}+1}^{d_g} \left(\bar{o}_h \cdot \left(o \left(\sum_{j=d_g+1}^{\infty} n_j \right) + \sum_{j=d_g+1}^{\infty} n_j \right) \right) + \sum_{h=1}^{\infty} \sum_{i=1}^{n_h} o_{h,i} \\
&= \sum_{g=1}^{\infty} \left(\sum_{h=d_{g-1}+1}^{d_g} \bar{o}_h \cdot \sum_{j=d_g+1}^{\infty} n_j \right) + \sum_{h=1}^{\infty} \sum_{i=1}^{n_h} o_{h,i} \\
&\leq \sum_{g=1}^{\infty} \left(3 \cdot (\delta_{g-1} + \delta_g) \cdot \sum_{j=d_g+1}^{\infty} n_j \right) + \sum_{h=1}^{\infty} \sum_{i=1}^{n_h} o_{h,i} \\
&= 3 \cdot \sum_{g=1}^{\infty} \left(\delta_g \cdot \left(\sum_{j=d_g+1}^{\infty} n_j + \sum_{j=d_{g+1}+1}^{\infty} n_j \right) \right) + \sum_{h=1}^{\infty} \sum_{i=1}^{n_h} o_{h,i} \\
&\leq 6 \cdot \sum_{g=1}^{\infty} \left(\delta_g \cdot \sum_{j=d_g+1}^{\infty} n_j \right) + \sum_{h=1}^{\infty} \sum_{i=1}^{n_h} o_{h,i}
\end{aligned}$$

$$\begin{aligned}
&\leq 6 \cdot \left(\sum_{g=1}^{\infty} \left(\delta_g \cdot \sum_{j=d_g+1}^{\infty} n_j + \sum_{r_\ell \in \mathcal{Z}_g} (p_\ell - t_g) \right) + \sum_{h=1}^{\infty} \sum_{i=1}^{n_h} o_{h,i} \right) \\
&= 6 \cdot \text{TEL}(\text{Optimal}; \mathcal{I}).
\end{aligned}$$

□

EC.3. Supplementary Materials for Section 5

EC.4. Supplementary Materials of Section 6

EC.4.1. Pseudocodes for LP-Based Methods

EC.4.2. Simulation Results and Analysis

This appendix presents a comprehensive empirical analysis of **Sorted-LP**, **Sorted-F (Swap)**, and **LP-Swap** algorithms through simulations on synthetically generated data. We employed five distinct distributions—Uniform, Normal, Binomial, Exponential, and Mixed—to model input (s_i) and output (o_i) lengths, with detailed parameters as follows.

Experimental Setup and Parameters

For all experiments, memory capacity $M = 100$ and maximum sequence lengths $s_{\max} = o_{\max} = 50$ were fixed. The distributions used are:

- **Uniform:** $s_i \sim \mathcal{U}(1, 51)$, $o_i \sim \mathcal{U}(1, 51)$.
- **Normal:** $\mu = 25$, $\sigma = 8.33$, $s_i, o_i \sim \mathcal{N}(\mu, \sigma^2)$ clipped to $[1, 50]$.
- **Binomial:** $s_i, o_i \sim \text{Binomial}(49, 0.5) + 1$.
- **Exponential:** $s_i, o_i \sim \text{Exp}(\lambda = 0.2)$ (scale=5) clipped to $[1, 50]$.
- **Mixed:** Designed to mimic real-world patterns in Section 7:
 - **Input sequences (s_i):**
 - * 80% exponentially distributed with $\lambda = 0.1$ (scale=10).
 - * 20% lognormally distributed with $\mu = \ln 40$, $\sigma = 0.25$.
 - * Values > 50 remapped to $\mathcal{U}(40, 50)$.

— **Output lengths (o_i):** Exponentially distributed with $\lambda = 0.2$ (scale=5) clipped to $[1, 50]$.

Figure EC.1 illustrates the distribution of input sequence lengths (s_i) for the Mixed dataset, highlighting its bimodal structure with predominantly short sequences and occasional longer requests.

Numerical Results

Table EC.1 summarizes the average total end-to-end latency (TEL) across all trials, providing the quantitative basis for our subsequent analysis.

Algorithm 2 Exact Optimal Request Selection via Dynamic Programming

```

1:  $n \leftarrow |\mathcal{I}|$ 
2: Initialize  $dp[k][m] \leftarrow \infty$  and  $path[k][m] \leftarrow \emptyset$  for  $k = 0..n$ ,  $m = 0..M$ 
3:  $dp[0][0] \leftarrow 0$ 
4: for each request  $r_i \in \mathcal{I}$  do
5:    $m_i \leftarrow s_i + o_i$ 
6:    $o_i \leftarrow$  output length
7:   for  $k \leftarrow n - 1$  downto 0 do
8:     for each  $m$  where  $dp[k][m] < \infty$  do
9:        $new_m \leftarrow m + m_i$ 
10:      if  $new_m \leq M$  then
11:         $new\_val \leftarrow dp[k][m] + o_i$ 
12:        if  $new\_val < dp[k+1][new_m]$  then
13:           $dp[k+1][new_m] \leftarrow new\_val$ 
14:           $path[k+1][new_m] \leftarrow path[k][m] \cup \{i\}$ 
15:        end if
16:      end if
17:    end for
18:  end for
19: end for
20:  $\mathcal{X}^* \leftarrow \emptyset$ ,  $F^* \leftarrow \infty$ 
21: for  $k = 1$  to  $n$  do
22:   for  $m = 0$  to  $M$  do
23:    if  $dp[k][m] < \infty$  then
24:       $F \leftarrow dp[k][m]/(k \times k)$ 
25:      if  $F < F^*$  then
26:         $F^* \leftarrow F$ 
27:         $\mathcal{X}^* \leftarrow \{r_i : i \in path[k][m]\}$ 
28:      end if
29:    end if
30:  end for
31: end for
32: return  $\mathcal{X}^*$ 

```

Algorithm 3 Local Swap Search

```

1: Sort  $\mathcal{I}$  by ascending  $s_i + o_i$ 
2:  $\mathcal{X} \leftarrow \emptyset$ ,  $mem \leftarrow 0$ 
3: for each  $r \in \mathcal{I}$  in sorted order do
4:   if  $mem + s_r + o_r \leq M$  then
5:      $\mathcal{X} \leftarrow \mathcal{X} \cup \{r\}$ 
6:      $mem \leftarrow mem + s_r + o_r$ 
7:   end if
8: end for
9:  $improved \leftarrow True$ 
10: while  $improved$  do
11:    $improved \leftarrow False$ 
12:    $currentF \leftarrow (\sum_{r \in \mathcal{X}} o_r) / |\mathcal{X}|^2$ 
13:   for each  $r_{out} \in \mathcal{X}$  do
14:     for each  $r_{in} \in \mathcal{I} \setminus \mathcal{X}$  do
15:        $\Delta_m \leftarrow (s_{in} + o_{in}) - (s_{out} + o_{out})$ 
16:       if  $mem + \Delta_m > M$  then
17:         continue
18:       end if
19:        $\Delta_o \leftarrow o_{in} - o_{out}$ 
20:        $newF \leftarrow (\sum_{r \in \mathcal{X}} o_r + \Delta_o) / |\mathcal{X}|^2$ 
21:       if  $newF < currentF$  then
22:          $\mathcal{X} \leftarrow (\mathcal{X} \setminus \{r_{out}\}) \cup \{r_{in}\}$ 
23:          $mem \leftarrow mem + \Delta_m$ 
24:          $improved \leftarrow True$ 
25:         break inner loop
26:       end if
27:     end for
28:   if  $improved$  then
29:     break
30:   end if
31: end for
32: end while
33: return  $\mathcal{X}$ 

```

Algorithm 4 Quantile Greedy Selection

```

1: Sort  $\mathcal{I}$  by ascending  $o_i$ 
2:  $sample\_size \leftarrow \max(1, \lfloor 0.5 \times |\mathcal{I}| \rfloor)$ 
3:  $sample \leftarrow$  random subset of  $\mathcal{I}$  with size  $sample\_size$ 
4:  $Q_p \leftarrow$  0.3-quantile of  $\{s_i + o_i \text{ for } r_i \in sample\}$ 
5:  $Q_o \leftarrow$  0.3-quantile of  $\{o_i \text{ for } r_i \in sample\}$ 
6:  $\mathcal{X} \leftarrow \emptyset, mem \leftarrow 0$ 
7: for each  $r \in \mathcal{I}$  in sorted order do
8:   if  $(s_r + o_r) \leq Q_p$  and  $o_r \leq Q_o$  and  $mem + s_r + o_r \leq M$  then
9:      $\mathcal{X} \leftarrow \mathcal{X} \cup \{r\}$ 
10:     $mem \leftarrow mem + s_r + o_r$ 
11:   end if
12: end for
13:  $remaining \leftarrow \mathcal{I} \setminus \mathcal{X}$ 
14: Sort  $remaining$  by ascending  $o_i / (s_i + o_i)$ 
15: for each  $r \in remaining$  in sorted order do
16:   if  $mem + s_r + o_r \leq M$  then
17:      $\mathcal{X} \leftarrow \mathcal{X} \cup \{r\}$ 
18:      $mem \leftarrow mem + s_r + o_r$ 
19:   end if
20: end for
21: return  $\mathcal{X}$ 

```

Table EC.1 Average total end-to-end latency across distributions

Distribution	Sorted-LP	Sorted-F (Swap)	LP-Swap	Requests (n)
Uniform	9763.0	9748.3	9771.4	100
Normal	9397.3	9416.9	9385.3	100
Binomial	10943.0	10696.7	10665.7	100
Exponential	6015.7	6016.9	6016.0	100
Mixed	22133.2	22100.1	22128.2	200

Key Observations

Through detailed analysis of algorithm execution—including batch formation dynamics, request sequencing patterns, and runtime scheduling decisions—we identify three notable empirical patterns:

Algorithm 5 Sorted-F+ \mathcal{A}_{\min} : Adaptive Scheduling under Prediction Uncertainty**Require:** Request set \mathcal{I} with prefill sizes $\{s_i\}$ and predicted intervals $\{\ell_i, u_i\}$; memory capacity M **Ensure:** Schedule minimizing total end-to-end latency

- 1: **Initialization:** Set $\tilde{o}_i \leftarrow \ell_i$ for all $i \in \mathcal{I}$ ▷ Optimistic initialization

- 2: **Phase 1: Batch Construction with Lower Bounds**
- 3: Run Phase 1 of Sorted-F (Algorithm 1) using \tilde{o}_i in place of o_i
- 4: Let \mathcal{I}' be the resulting ordered request sequence

- 5: **Phase 2: Adaptive Scheduling Execution**
- 6: $t \leftarrow 0$, $\mathcal{R}^{(0)} \leftarrow \mathcal{I}'$, $\mathcal{V}^{(0)} \leftarrow \emptyset$
- 7: **while** $\mathcal{R}^{(t)} \neq \emptyset$ **or** $\mathcal{V}^{(t)} \neq \emptyset$ **do**
- 8: $t \leftarrow t + 1$
- 9: **for** $r_i \in \mathcal{V}^{(t-1)}$ **do** ▷ Update running estimates
- 10: $\tilde{o}_i \leftarrow \max\{\tilde{o}_i, t - p_i\}$
- 11: **end for**
- 12: Remove completed requests: $\mathcal{V}^{(t)} \leftarrow \{r_i \in \mathcal{V}^{(t-1)} : t - p_i < \tilde{o}_i \text{ or } r_i \text{ not yet terminated}\}$

- 13: **Admission Step:** Attempt to add pending requests to active set
- 14: Run admission logic of Phase 2 of Sorted-F using current $\{\tilde{o}_i\}$ values
- 15: Let $\mathcal{U}^{(t)}$ be the set of newly admitted requests; set $p_i \leftarrow t$ for $r_i \in \mathcal{U}^{(t)}$

- 16: **Eviction Step:** Resolve memory overflow if necessary
- 17: **while** $M(\mathcal{V}^{(t)} \cup \mathcal{U}^{(t)}, \{\tilde{o}_j\}) > M$ **do** ▷ Ordered eviction from \mathcal{A}_{\min}
- 18: $r^* \leftarrow \arg \min_{r_i \in \mathcal{V}^{(t)} \cup \mathcal{U}^{(t)}} \tilde{o}_i$ ▷ Evict request closest to completion
- 19: $\mathcal{V}^{(t)} \leftarrow \mathcal{V}^{(t)} \setminus \{r^*\}$; $\mathcal{U}^{(t)} \leftarrow \mathcal{U}^{(t)} \setminus \{r^*\}$
- 20: Return r^* to pending queue $\mathcal{R}^{(t)}$ with updated \tilde{o}_{r^*}
- 21: **end while**

- 22: $\mathcal{R}^{(t)} \leftarrow \mathcal{R}^{(t)} \setminus \mathcal{U}^{(t)}$
- 23: $\mathcal{V}^{(t)} \leftarrow \mathcal{V}^{(t)} \cup \mathcal{U}^{(t)}$
- 24: PROCESSONESTEP($\mathcal{V}^{(t)}$)
- 25: **end while**

Algorithm 6 Sorted-LP

```

1: Solve Relaxed-LP and obtain an optimal fractional solution  $x_{i,t}^*$  for all  $i \in [n], t \in [\bar{T}]$ 
2: for each  $i \in [n]$  do
3:   Compute  $y_i \leftarrow \sum_{t \in [\bar{T}]} t \cdot x_{i,t}^*$ 
4: end for
5: Sort all requests  $r_i \in \mathcal{I}$  in ascending order of  $y_i$  to obtain an ordered list  $\mathcal{I}'$ 
6:  $t \leftarrow 0, \mathcal{R}^{(0)} \leftarrow \mathcal{I}', \mathcal{V}^{(0)} \leftarrow \emptyset$ 
7: while  $\mathcal{R}^{(t)} \neq \emptyset$  or  $\mathcal{V}^{(t)} \neq \emptyset$  do
8:    $t \leftarrow t + 1$ 
9:    $\mathcal{U}^{(t)} \leftarrow \emptyset$ 
10:   $\mathcal{V}^{(t)} \leftarrow \{r_j \in \mathcal{V}^{(t-1)} : p_j + o_j \geq t\}$ 
11:  for  $r_i \in \mathcal{R}^{(t-1)}$  in order do
12:    tentatively set  $p_i \leftarrow t$ 
13:     $\hat{\mathcal{U}} \leftarrow \mathcal{U}^{(t)} \cup \{r_i\}$ 
14:    if  $M(\mathcal{V}^{(t)} \cup \hat{\mathcal{U}}, p_j + o_j) \leq M, \forall r_j \in \mathcal{V}^{(t)} \cup \hat{\mathcal{U}}$  then
15:       $\mathcal{U}^{(t)} \leftarrow \hat{\mathcal{U}}$ 
16:    else
17:      break
18:    end if
19:  end for
20:   $\mathcal{R}^{(t)} \leftarrow \mathcal{R}^{(t-1)} \setminus \mathcal{U}^{(t)}$ 
21:   $\mathcal{V}^{(t)} \leftarrow \mathcal{V}^{(t)} \cup \mathcal{U}^{(t)}$ 
22:  PROCESSONESTEP( $\mathcal{V}^{(t)}$ )
23: end while

```

1. **LP's preference for short-output requests:** The Sorted-LP approach consistently prioritizes requests with shorter output lengths (o_i), even when their input sizes (s_i) are substantial. This behavior appears related to the LP formulation's relaxation, where fractional $x_{i,t}$ variables reduce the perceived cost of memory blocking by large inputs. Consequently, minimizing output latency dominates scheduling decisions, which can lead to suboptimal memory allocation when large-input requests are scheduled early.

Algorithm 7 LP-Swap

1: Solve Relaxed-LP and obtain $x_{i,t}^*$ for all $i \in [n], t \in [\bar{T}]$; set $y_i \leftarrow \sum_{t \in [\bar{T}]} t x_{i,t}^*$ for all $i \in [n]$

Helper: FEASIBLE(\mathcal{S}) $\equiv (M(\mathcal{S}, p_j + o_j) \leq M, \forall r_j \in \mathcal{S})$

2: $\mathcal{I}' \leftarrow \emptyset$

3: **while** $\mathcal{I} \neq \emptyset$ **do**

4: Sort \mathcal{I} by increasing y_i

5: $\mathcal{X}_{\text{init}} \leftarrow \emptyset, mem \leftarrow 0$

6: **for** each $r \in \mathcal{I}$ in this order **do**

7: **if** $mem + s_r + o_r \leq M$ **then**

8: $\mathcal{X}_{\text{init}} \leftarrow \mathcal{X}_{\text{init}} \cup \{r\}; mem \leftarrow mem + s_r + o_r$

9: **end if**

10: **end for**

11: $\mathcal{X}^* \leftarrow \text{LOCALSWAP}(\mathcal{X}_{\text{init}}, \mathcal{I}, M)$

12: Sort \mathcal{X}^* by nondecreasing o_i

13: Append \mathcal{X}^* to \mathcal{I}'

14: $\mathcal{I} \leftarrow \mathcal{I} \setminus \mathcal{X}^*$

15: **end while**

16: $t \leftarrow 0; \mathcal{R}^{(0)} \leftarrow \mathcal{I}'; \mathcal{V}^{(0)} \leftarrow \emptyset$

17: **while** $\mathcal{R}^{(t)} \neq \emptyset$ **or** $\mathcal{V}^{(t)} \neq \emptyset$ **do**

18: $t \leftarrow t + 1; \mathcal{U}^{(t)} \leftarrow \emptyset; \mathcal{V}^{(t)} \leftarrow \{r_j \in \mathcal{V}^{(t-1)} : p_j + o_j \geq t\}$

19: **for** $r_i \in \mathcal{R}^{(t-1)}$ in order **do**

20: **tentatively set** $p_i \leftarrow t$

21: **if** FEASIBLE($\mathcal{V}^{(t)} \cup \mathcal{U}^{(t)} \cup \{r_i\}$) **then**

22: $\mathcal{U}^{(t)} \leftarrow \mathcal{U}^{(t)} \cup \{r_i\}$

23: **else**

24: **break**

25: **end if**

26: **end for**

27: $\mathcal{R}^{(t)} \leftarrow \mathcal{R}^{(t-1)} \setminus \mathcal{U}^{(t)}; \mathcal{V}^{(t)} \leftarrow \mathcal{V}^{(t)} \cup \mathcal{U}^{(t)}$

28: PROCESSONESTEP($\mathcal{V}^{(t)}$)

29: **end while**

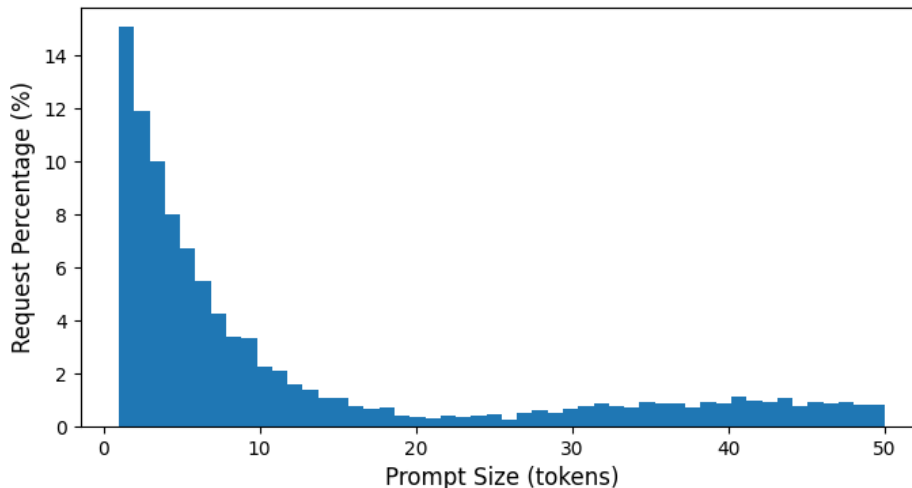


Figure EC.1 Distribution of input sequence lengths (s_i) in the Mixed dataset configuration

2. **Swap’s balancing effect:** The swap mechanism effectively counteracts this bias by considering both input and output sizes during local exchanges. This dual consideration produces more balanced schedules that better account for memory constraints, particularly in distributions where naive prioritization of short outputs could allow memory-intensive requests to cause disproportionate blocking.

3. **LP+Swap synergy and performance:** The hybrid LP-Swap approach combines LP’s global optimization perspective with swap’s local refinement capabilities. While pure swap achieves marginally better results in the Mixed distribution (designed to simulate real-world data), LP-Swap demonstrates competitive performance across all tested distributions. This consistent adaptability suggests that integrating both techniques offers a promising direction for developing robust schedulers that maintain effectiveness under diverse request patterns.

These empirical patterns provide motivation for further investigating hybrid scheduling strategies, which we pursue with real-world datasets in Section 7.

EC.5. Supplementary Materials of Section 7

Figure EC.2 is a refined figure of Figure 8, which only compares the two curves (Sorted-F and LP-Swap) which almost overlap with each other.

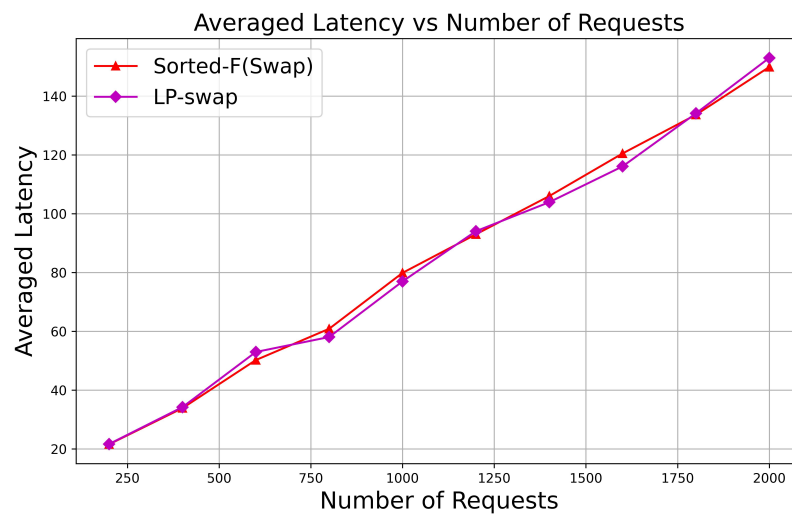


Figure EC.2 Averaged latency between Sorted-F and LP-Swap